SAPIENZA
UNIVERSITÀ DI ROMA

Modelling, simulation and analysis of the electrical distribution system of a nuclear fusion reactor and its connection to the grid

University of Rome "La Sapienza"
Doctoral Degree in Engineering and Applied Science for Energy and Industry (XXXVI cycle)

Marzia Caldora
ID number 1943602

Advisor
Prof. Maria Carmen Falvo

Co-Advisor
Eng. Alessandro Lampasi
Eng. Roberto Romano

Academic Year 2022/2023

Thesis defended on 23 September 2024
in front of a Board of Examiners composed by:

Prof. Giorgio Sulligoi, Full Professor, University of Trieste (chairman)

Prof. Filippo Spertino, Full Professor, Polytechnic University of Turin (secretary)

Prof. Aguinaldo Fraddosio, Associate Professor, Polytechnic University of Bari (member)

Modelling, simulation and analysis of the electrical distribution system of a nuclear fusion reactor and its connection to the grid

PhD thesis. Sapienza University of Rome

This thesis has been typeset by LaTeX and the Sapthesis class.

Author's email: marzia.caldora@uniroma1.it

A Bianca,
niente sarebbe stato possibile
senza il tuo supporto.

A ciò che valgo.

Abstract

Nuclear fusion represents an attractive and sustainable source of clean energy for the future. However, its successful implementation relies heavily on a robust and efficiently managed electrical distribution network. This thesis explores the development of simulation models for analyzing such a network supporting a nuclear fusion reactor. The research, conducted between 2020 and 2023, focuses on assessing network connectivity, potential impacts, and safety aspects during operation.

Advanced simulation tools like PowerFactory were employed to model and verify the proposed distribution network design, ensuring its efficiency and reliability. The thesis addresses both the technical intricacies of the design and the paramount importance of operational safety. By modeling various operational scenarios and their implications, this research contributes valuable insights towards achieving a safe and efficient nuclear fusion energy distribution network.

The context of this research is framed within the ambitious nuclear fusion project, requiring significant resources for large-scale power generation. The EUROfusion Roadmap outlines a strategic path for pursuing fusion energy in Europe, with key milestones like ITER (completion by 2030) and DEMO projects. These international collaborations aim to demonstrate the feasibility and safety of nuclear fusion for electricity production.

This thesis specifically focuses on modeling the electrical distribution network for a nuclear fusion power plant, with a view towards ensuring the safety and feasibility of design choices for projects like DTT and DEMO. The research delves into various aspects, including socioeconomic considerations, nuclear physics, tokamak operation, and simulation model development for the electrical distribution system. Dedicated chapters explore these topics in detail.

Chapter 1 provides an overview of the socioeconomic implications of nuclear fusion exploitation for electricity generation, together with the fundamental physics behind the process. An introduction of the technologies developed so far is also given, with a particular focus on tokamak devices.

Chapter 2 delves with the requirements of a Nuclear Fusion Power Plant (NFPP) both in terms of the necessary component systems and in terms of standards and regulations governing its operations.

Chapter 3 centers on optimizing the design of a nuclear fusion facility's internal electrical distribution network. To achieve this goal, simulation models were developed and applied to analyze various aspects across two case studies. The analyses included preliminary design, sizing, operation analysis, and progress in the design of the electrical distribution system for the DTT project. Additionally, a Probabilistic Power Flow (PPF) analysis is employed to define and quantify the uncertainties associated with power demand and absorption within the DEMO plant's electrical grid.

Conclusions are reported in *Chapter 4*.

The publications related to the work carried out during the PhD course can be found in the following references: [1–5].

Contents

List of Figures

List of Tables

Acronym List

ACER	Agency for the Cooperation of Energy Regulators
ALARA	As Low As Reasonably Achievable
AUX	Auxiliaries
BEN	Binding Energy per Nucleon
BoP	Balance of Plant
BUI	Buildings
CCS	Carbon Capture and Storage
CRYO	Cryoplant and Cryodistribution
CS	Central Solenoid
DC	Direct current
DEMO	DEMOnstration Power Plant
DIA	Diagnostics
DPF	Deterministic Power Flow
DSO	Distribution System Operator
DTT	Divertor Tokamak Test
DV	Divertor Coil
ECRH	Electron Cyclotron Resonance Heating
EDG	Emergency Diesel Generator
EDS	Electrical Distribution System
EF	Error Fields
EFDA	European Fusion Development Agreement
EFCC	Error Field Correction Coil
ELL	Electrical Load List
ELM	Edge Localized Mode

EMRIO Extended Multi-Regional Input-Output

ENS Electrical Network System

ENTSO-E European Network of Transmission System Operators for Electricity

ETM EFDA TIMES Model

FDU Fast Discharge Unit

FTU Frascati Tokamak Upgrade

GCAM Global Change Analysis Model

HCD Heating and Current Drive

HVDC High Voltage Direct Current

HVN High Voltage Network

HVS High Voltage System

IAEA International Atomic Energy Agency

ICRH Ion Cyclotron Resonance Heating

IO Input-Output

IOA Input-Output Approach

ITER International Thermonuclear Experimental Reactor

JET Joint European Torus

LC Load Center

LCOE Levelized Cost of Electricity

LDNE Linearized Dynamic New Earth

LIFE Laser Inertial Fusion Energy

MCS Monte Carlo Simulation

MHD Magneto Hydro Dynamic

MLVN Medium and Low Voltage Network

MRIOT Multiregional Input-Output Table

NBI Neutral Beam Injection

NC RfG Network Code Requirements for Generators

NFPP Nuclear Fusion Power Plant

NG National Grid

NIF National Ignition Facility

PCS	Power Conversion System
PDF	probability distribution function
PES	Plant Electrical System
PFC	Poloidal Field Coil
PGM	Power Generating Module
PHTS	Primary Heat Transfer System
PL	Project Leader
PPEN	Pulsed Power Electrical Network
PPF	Probabilistic Power Flow
PPM	Power Park Module
PSS	Power Supply System
PTG	Power Transmission Grid
PV	Photovoltaic
RES	Renewable Energy Source
RF	Radio Frequency
RM	Remote Maintenance
RMS	Root Mean Square
SIC	Safety Important Component
SOL	Scrape-Off Layer
SR	Safety Relevant
SSCs	Structures, Systems and Components
SSEN	Steady-State Electrical Network
SSP	Shared Socioeconomic Pathway
SY PGM	Synchronous Power Generating Module
TBD	To Be Defined
TBM	Test Blanket Module
TER	Tritium Extraction and Removal
TFC	Toroidal Field Coil
TFV	Tritium, Fuelling, Vacuum
TG	Turbine Generator

TSO Transmission System Operator

VNS Volumetric Neutron Source

WCLL Water Cooled Lithium Lead

WIOD World Input Output Database

Chapter 1

Introduction to Nuclear Fusion

The increasing global awareness of climate change and the depletion of fossil fuel sources have driven research in the energy sector. While significant progress has been made in sustainable renewable energy sources like Photovoltaic (PV) and wind, challenges arise from their decentralized nature and grid impact due to variability. Maintaining grid stability requires voltage and frequency regulation, posing challenges with high PV and wind penetration [6]. PV systems, though popular, lack reactive power support, leading to voltage issues. Wind farms provide some reactive power, but not enough for full voltage regulation. Both technologies lack the inertia needed for frequency control, necessitating fast response storage systems for grid stability.

As these inertialess systems grow, research into non-CO_2 emitting base generation becomes crucial to provide grid inertia and reliability. The rising global electricity demand underscores the need for high-power generation plants. However, conventional fuels are not sustainable, leading to substantial investments in nuclear fusion research as a solution that combines high-power generation with environmental sustainability.

However, the challenges inherent in fusion encompass a complex interweaving of scientific and technological hurdles. This has motivated the European fusion community to develop a comprehensive, ambitious yet pragmatic roadmap whose central vision is to deliver fusion-generated electricity to the grid by the mid-21st century, achieved through a carefully integrated science, technology, and engineering program.

Initially outlined in 2012 by EUROfusion's predecessor, the European Fusion Development Agreement (EFDA), the Roadmap to the realization of fusion energy [7] is a foundational document that defines the essential framework for advancing nuclear fusion as a viable energy source. The missions and objectives articulated in this roadmap encompass critical aims such as enhancing fusion material research, designing viable blanket modules, formulating energy-efficient fusion scenarios, developing cutting-edge technologies to manage extreme plasma conditions, and ensuring the safety and reliability of fusion power.

This chapter offers a general overview of the socioeconomic implications of nuclear fusion, focusing on its potential impact on energy markets, environmental sustainability, and global energy policies. Fundamentals of nuclear fusion theory are also introduced, along with a brief overview of existing fusion technologies.

1.1 Socioeconomic Implications of Nuclear Fusion: an Overview

Governments and businesses are increasingly committed to ambitious decarbonization targets, yet energy markets cope with extreme volatility fueled by geopolitical tensions and a post-

COVID-19 rebound in energy demand. The conflict in Ukraine, among other factors, has resulted in significant spikes in energy prices, emphasizing concerns about supply security and affordability within an already constrained market.

In 2021, global energy demand and emissions rose by 5%, nearly reaching pre-COVID-19 levels at approximately 33 gigatons of energy-related CO_2 equivalent. Currently, power generation contributes about 30% of global CO emissions [8]. To achieve the Paris Agreement's full decarbonization target by 2050 [9] and the emission reduction goals outlined in the "Global Warming of 1.5°C" IPCC Special Report [10], many governments and utilities are transitioning away from fossil fuels to embrace renewable-energy technologies, aiming for a zero-carbon energy grid. While short-term challenges include market volatility and geopolitical complexities, the long-term economics of renewable-power sources are poised to drive substantial investments. As power consumption is projected to triple by 2050 [8], ensuring all added generation is zero carbon becomes imperative.

Renewable energy from wind and solar presently stands as the most cost-efficient form of new zero-carbon electrical generation. By 2030, it is expected to be the lowest-cost option in most markets. Despite their cost efficiency, wind and solar have limitations, being non-dispatchable and relying on external variables for power generation. Dispatchable zero-carbon energy forms, like geothermal or tidal power, show promise but are generally more expensive and less technologically mature.

Nuclear fusion, once considered a distant dream, has made significant technological advancements in recent years. Offering the potential for dispatchable, zero-carbon energy with no long-lived nuclear waste, it has emerged as a promising candidate to address the global energy crisis. However, harnessing the power of fusion will not be without its challenges and opportunities.

The successful transition towards fusion power generation has the potential to revolutionize the global energy landscape, impacting energy security, reducing greenhouse gas emissions, and influencing regional and global economies. This transition, however, also carries the prospect of disruptive changes in the energy sector, with repercussions across various socio-economic spheres.

The implementation of fusion reactors requires a substantial upfront investment, particularly during the construction phase. However, this initial outlay is anticipated to yield long-term positive economic impacts including the creation of jobs and associated economic growth. The employment potential is extensive, ranging from direct personnel during operation to the induced effects of the technology's implementation across various sectors.

Despite its high initial costs, fusion's Levelized Cost of Electricity (LCOE) advantage over fossil fuels contributes to long-term sustainability. In addition, the projected decline in costs as more fusion plants are built further strenghtens its economic viability.

Understanding the economic potential of fusion energy is complex due to the numerous uncertainties involved, ranging from individual power plant considerations to the broader dynamics of the global energy system. The future success of fusion as an electricity source relies not only on its cost trajectory but also on the evolving global electricity market. Its market share will depend on factors such as climate change policies, the relative costs of competing technologies, and public acceptance.

1.1.1 Costs of Fusion Electricity

As shown in Figure 1.1, the cost of fusion electricity is influenced mainly by capital cost and the operational hours per year of the plant [11].

The LCOE represents an important indicator, being the total cost of building and running

a plant throughout its lifetime, divided by the kilowatt hours of energy generated during that period [12]. It is typically measured in mill/kWh[1] and is defined as specified in Eq. 1.1.

$$\mathrm{LCOE} = \frac{\sum_{t=1}^{n} \frac{I_t + M_t + F_t}{(1+r)^t}}{\sum_{t=1}^{n} \frac{E_t}{(1+r)^t}} \tag{1.1}$$

Where:

- I_t is the investment expenditures in the year t,
- M_t is the operations and maintenance expenditures in the year t,
- F_t is the fuel expenditures in the year t,
- E_t is the electrical energy generated in the year t,
- r is the discount rate,
- n is the expected lifetime of the system.

Similar to its fission counterpart, the total expenses of a fusion power plant are predominantly related to the initial capital outlay. The cumulative kilowatt hours produced over the plant's lifespan are contingent on factors such as its size, the annual operational hours, and the efficiency in converting thermal energy from fusion into electricity. Numerous estimates exist for the capital cost of a fusion plant [11, 13–15].

Cost models typically predict a specific rate of cost reduction with each additional unit deployed, due to a phenomenon known as "technological learning". This means that as we gain experience and knowledge from each new plant, we can build subsequent ones cheaper and more efficiently. For instance, increasing maturity may enhance the efficiency of converting thermal fusion energy into electricity, potentially doubling the efficiency from 30% to 60%. The efficiency is particularly influenced by the blanket's temperature, where maintaining a higher temperature difference between the blanket and the environment results in increased electricity generation efficiency.

For comprehensive electricity cost estimation, the initial capital cost needs to be "annualized", i.e. transformed into a yearly cost, by multiplying it by a percentage factor (typically 15% per year) which accounts for borrowing costs, depreciation, insurance and taxes [11].

However, plants do not operate continuously for an entire year, and the assumption about the number of hours the plant runs annually becomes a variable in cost estimates. Fusion, being a capital-intensive technology, generally requires nearly continuous operation to stay competitive. A crucial factor for fusion plants is "scheduled component replacement", impacting their availability. Components near the fusion plasma, such as the first wall, blanket, and divertor, degrade and require replacement multiple times due to irradiation by fusion neutrons and charged particles. Replacement periods, particularly for divertor and blanket replacement, are estimated at four and six months, respectively, with additional cooling and conditioning periods before the plant can resume power production [16]. The durability of components requiring replacement is crucial for the cost of fusion electricity which explains why fusion's priority lies in developing and demonstrating materials that can endure the fusion environment for extended periods. In fission plants, analogous materials have enabled approximately 90% operational time with a single yearly shutdown. While the

[1] 1 mill is equal to 1/1000 of a U.S. dollar, or 1/10 of one cent. Mills per kilowatt-hour (kWh) are equivalent to dollars per megawatt-hour (MWh).

pressure vessel in a fission plant, the most challenging component to replace, remains intact for the plant's lifetime, fusion neutrons, being more energetic, cause more damage. As shown in Figure 1.1, capital expenditure dominates the cost structure, accounting for 73%. This includes initial investments in plant construction, components such as Magnets and Cooling Systems, and building constructions and site preparation. Recurring operational costs constitute the remaining 27%, encompassing Divertor Replacement (12%), Blanket/First Wall Replacement (4%), and ongoing Operation and Maintenance (9%). Additional expenses, such as fuel and decommissioning, are considered negligible (2%). The cost of handling regenerated tritium, a fuel byproduct, is likely allocated to the operation and maintenance category due to its recurring nature.

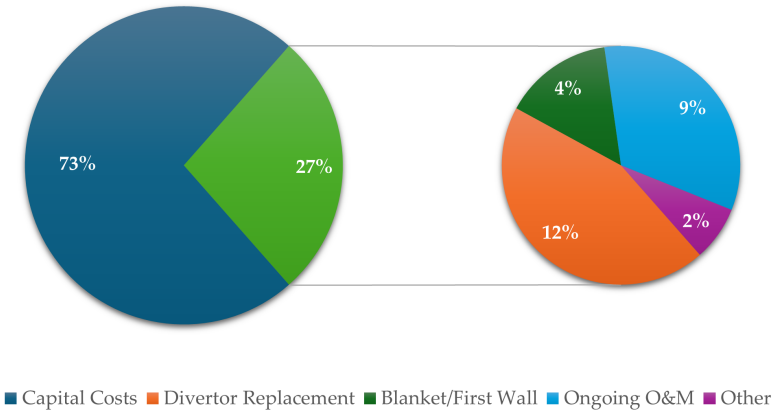

Figure 1.1. Estimated percentage breakdown of the total cost of electricity generation in a tokamak fusion power plant.

Despite the deep uncertainty about fusion's likely future cost, the economic competitiveness of fusion energy in the global context has been explored by high level modeling studies, many of which are summerized in Table 1.1 [17].

While the literature on engineering, physics and technical aspects of the development of nuclear energy, components is extensive and mature, the economic scope has also been covered in last decades although most of these studies have been focused on the cost of electricity. However, socioeconomic assessments, addressing value added and employment creation related to fusion power deployment, are scarcer.

The following paragraphs offer a comprehensive introduction to three significant socioeconomic studies assessing the overall impact of fusion on the global energy system. Their selection is motivated by their crucial contributions to comprehending the broader implications for the global energy system since they provide valuable insights, employ robust methodologies and comprehensive perspectives making them particularly pertinent for an in-depth examination of the multifaceted aspects associated with fusion's influence.

1.1.2 The Global Change Analysis Model

The [21] is a study employing the GCAM, an integrated model developed at the Joint Global Change Research Institute, University of Maryland, designed to assess climate change policies

Table 1.1. Review of studies employing energy systems models to assess the potential role of fusion energy.

Authors	Scope	Model	Major Results
Vaillancourt et al., [18]	Penetration level of nuclear power, encompassing fusion energy, under different assumptions regarding technological factors and external limitations on nuclear advancement, alongside public attitudes towards two climate change scenarios (CO_2 concentrations at 450 ppmv and 550 ppmv by 2100)	World-TIMES	The global nuclear fusion capacity is projected to reach 1500 GW by 2100 under the scenario targeting a CO_2 concentration of 450 ppmv. This capacity is expected to be primarily developed in the USA and Western Europe, with anticipated capacities of 485 GW and 375 GW respectively by 2100. Additional contributions are expected from China, India, and the Former Soviet Union, albeit to a lesser extent.
Muehlich and Hamacher [19]	Potential influence of the transportation industry on the integration of fusion energy into the 21st-century energy landscape	EFDA-TIMES	Fusion power could potentially contribute up to 50% of total electricity generation by 2100 in the scenario aiming for 450 ppm of CO_2 concentration.
Gnansounou and Bednyagin, [20]	The worldwide potential for implementing fusion power by developing multi-regional, long-term electricity market scenarios extending to the year 2100.	PLANELEC-Pro	Potential contribution of fusion to the reduction of global CO_2 emissions from power generation is estimated at 1.8–4.3%.
Turnbull et al., [21]	The interplay among technology, climate considerations, and public policy, alongside an analysis of factors influencing the expansion of fusion energy	Global Change Analysis Model (GCAM)	The discounted value of the fusion option is estimated to range from hundreds of billions to trillions of dollars.
Tokimatsu et al., [22]	Breakeven price and the potential electricity supply of nuclear fusion energy in the 21st century	Linearized Dynamic New Earth (LDNE)	The breakeven prices range between 65 to 125 mill kW^{-1} h^{-1}, and the anticipated contribution of electricity generated by current tokamak-type nuclear fusion reactors by 2100 is expected to remain below 30% under the constraint of 550 ppmv CO_2 concentration.
Tokimatsu et al., [23]	Roles of nuclear fusion when breakeven prices are achieved	LDNE	There is a strong likelihood that current-design nuclear fusion reactors could become economically viable for integration into energy systems by around 2050–2060, under constraints on CO_2 concentration.
Cabal et al., [24]	Contributions of fusion technologies in the global electricity system in the long term	EFDA TIMES Model (ETM)	The fusion share in the global electricity system is 1–42% in 2100.

and technology strategies, exploring their impact and costs on mitigating climate change, including interactions with terrestrial systems [25, 26].

The model takes as inputs the performance of the economy, carbon-cycle science, climate policy, and the costs of competing energy technologies including fusion. Therefore, it generates predictions for future energy markets across 14 geopolitical regions, providing insights at five-year intervals spanning from 2015 to 2095. At each time step, the demand for electricity is met by a diverse range of energy technologies.

The first fusion power plant is assumed to become operational in 2035, with at least ten plants running by 2050 and at least 100 plants online by 2065.

Assumptions are also made on costs: median capital costs decline as fusion deployment progresses, and the unit cost is expected to decrease as more units are constructed. Moreover, fission and fusion costs are considered comparable.

Availability is another key factor: the plant is assumed to operate 90% of the time, minimizing the downtime for replacing irradiated reactor components.

Since the analysis results sensitive to the assumptions made, fusion becomes competitive under specific conditions. Notably the outcomes are strongly dependant on factors such as the commencement date and initial cost of the first commercial fusion plant, the rate of unit cost reduction through learning, and the costs and constraints of competitors.

Among the various Scenarios explored, two (the most and the less favourable to fusion) are considered the most representative and compared in the two panels of Figure 1.2 [27]. The numbers at the right (in percent) are the shares of total electricity production in 2095 for five bracketed power sources; from top to bottom, these are intermittent renewables, non-intermittent renewables, nuclear fission, fossil sources with and without Carbon Capture and Storage (CCS), and nuclear fusion.

In the initial scenario (depicted in the first panel), the baseline situation is characterized by the absence of climate policies. Both fission and CCS options are fully accessible, leading to fusion capturing a modest 4% market share by the year 2095. On the contrary, Scenario II (depicted in the second panel) introduces climate policies and implements a carbon price. This results in a substantial surge in fusion's market share, reaching 32% and generating 41 trillion kilowatt-hours, ten times more than the base Scenario I. The scenarios also highlight the impact of carbon targets, as evidenced by global electricity demand reaching 120 trillion kilowatt-hours in Scenario II, where a 450 parts per million (ppm) target is in place, compared to 90 trillion kilowatt-hours in Scenario I without any target. Notably, despite fusion having higher costs than fission in Scenario II, its increased market share highlights the profound influence of climate policies on shaping energy dynamics.

The study underscores two key outcomes. Firstly, in the absence of a carbon target and without explicit penalties on fusion's competitors, its share of electricity by the end of the century is marginal. Secondly, the imposition of a carbon target along with restrictions on fission and CCS significantly amplifies fusion's market share.

1.1.3 The DNE21+ Model

The DNE21+ model [28] is a linear programming model which minimizes the world energy system cost. Specifically, it is designed for a comprehensive and quantitative assessment of the international framework and targets related to global warming beyond 2013. It focuses on evaluating the effectiveness of specific countermeasure technologies, utilizing detailed technology data from various sectors worldwide. This model serves as an advanced analytical tool, enabling a thorough assessment of both global and sector-specific approaches to address climate change.

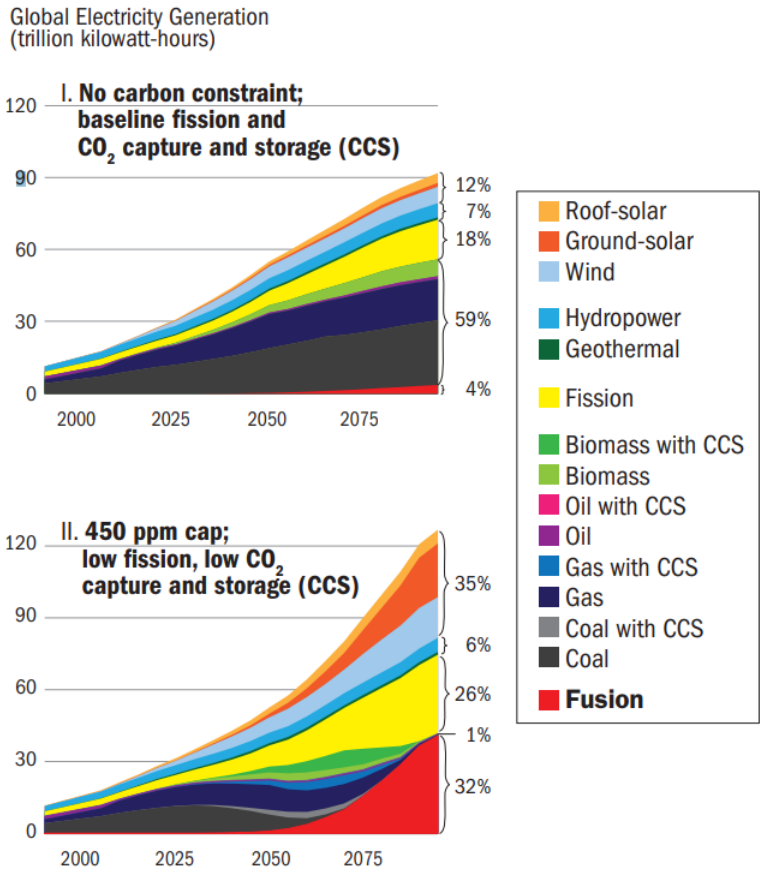

Figure 1.2. Production of global electricity in the 21st century, by source, when fusion is an option.

The model represents regional differences dividing the world into 54 regions, and assesses energy technologies which are bottom-up modelled in detail.

In [17], the potential contribution of fusion energy to low-carbon development, aligned with the Paris Agreement, was assessed. The analysis considered uncertainties in future socioeconomic development, the probability of achieving the 2°C target, and the development of commercial fusion power plants. A global energy systems model was employed to analyse energy systems from 2000 to 2100, incorporating different socioeconomic scenarios, global CO_2 emission pathways, and fusion power plant economics.

As illustrated in Figure 1.3, the study utilizes five Shared Socioeconomic Pathways (SSPs) to evaluate climate change impacts, incorporating qualitative narratives of various factors. Three SSPs – Sustainability (SSP1), Middle of the Road (SSP2), and Fossil Fuel Development (SSP5) – were employed to represent different challenges for climate change mitigation.

Regarding long-term targets, the study considered the Paris Agreement's goal to limit the global average temperature increase and employed four representative global CO_2 emissions pathways based on different climate sensitivities and temperature trajectories. Three types of global mean surface temperature trajectories were employed: overshooting 2°C before 2100 but declining below 2°C by 2100, stabilization below 2°C increase without exceeding it, and stabilization at 450-ppmv CO_2 equivalent by 2100. These pathways were calculated using the MAGICC climate change model [29], employing climate sensitivities of 3.0°C and 2.5°C. All pathways align with the 2°C target [30] (Figure 1.4) based on current scientific understanding.

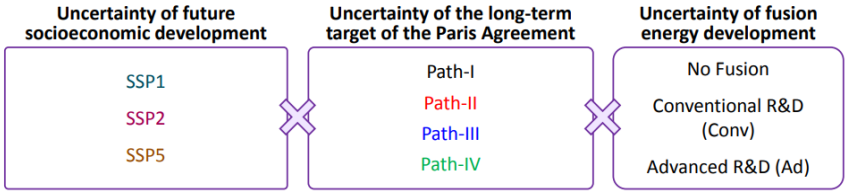

Figure 1.3. Analytical framework and uncertainties considered in the study.

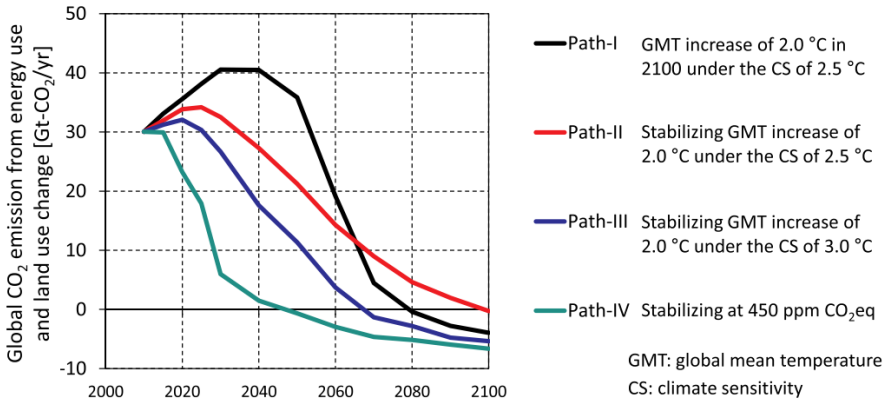

Figure 1.4. Global CO_2 emissions pathways corresponding to the 2 °C target.

The competitiveness of fusion power plants was assessed in the context of other zero-emission energy sources, particularly addressing the controversies surrounding nuclear fission energy (low public acceptance).

Two types of commercial fusion power plants were assumed, considering different capital costs (Table 1.2), capacity expansion constraints (influenced by initial tritium loading and the location of fusion plants – Figure 1.5), and plasma performance factors (measured by the normalized beta value[2]) [31]. The study fixed the capacity expansion at a linear rate. Parameters are of course tentative and subject to revision based on updates in fusion energy development scenarios.

Table 1.2. Assumptions on fusion power plants according to the DNE21+ model for conventional and advanced R&D scenarios.

	Conventional R&D	**Advanced R&D**
Capital costs per unit [US$2000/W]	8.5	6.6
Plant availability [%]	90	90
Life time [yr]	40	40
Annual expense ratio [%]	12	12
Fuel and back-end costs [US$2000/MWh]	2.0	2.0
Capacity constraint	Maximum limit of annual capacity introduction of 2 GW/yr by region.	

[2]The normalized beta β_N is an important dimensionless parameter that indicates how close the plasma is to the stability limit imposed by the magnetic fields. Higher β_N values indicate a more efficient confinement and greater potential for sustained fusion reactions.

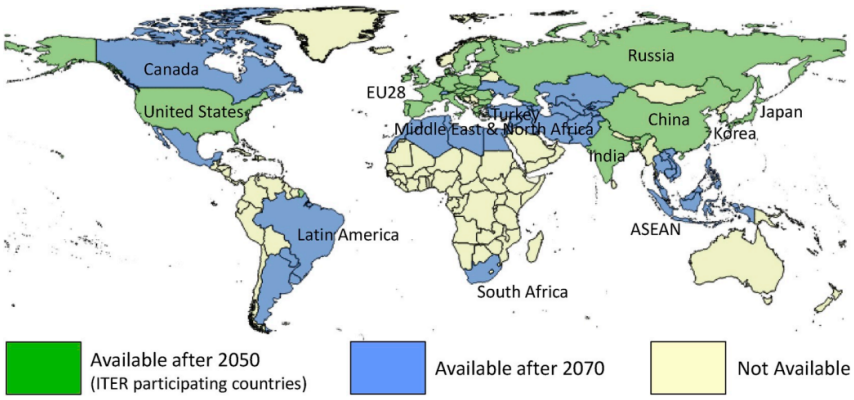

Figure 1.5. Assumption on availability of fusion energy per region according to the DNE21+ model.

The DNE21+ model study concludes that fusion power generation could significantly contribute to global low-carbon development by 2100. Emphasizing the need for drastic decarbonization, the study suggests fusion power plants could play a crucial role, especially in countries with limited zero-emission potential. Cost-efficient fusion plants, if developed through enhanced R&D, could extend their impact to regions like European Union, India and China. However, further cost reductions and innovative designs are essential for effectiveness, acknowledging uncertainties in future energy systems. The study highlights key directions for global energy systems: decarbonization, digitalization and decentralization, emphasizing the importance of long-term investments and clear strategies for social acceptance. It explores an alternative option of fusion energy for hydrogen production and provides valuable insights for future strategic planning, stressing the need for stakeholder involvement and comprehensive energy policies aligned with the energy trilemma.

1.1.4 The EMRIO Model

The [32] adopts an EMRIO approach to comprehensively assess the socioeconomic and environmental implications of nuclear fusion. This model takes into consideration various factors, including total production of goods and services, value-added creation, employment generation, and CO_2 emissions. The analysis focuses on the investment phase of a 1.45 GW fusion power plant project in Europe, also considering induced effects that may play a role in economic growth, employment and CO_2 emissions across different regions of the world.

This analytical framework combines the traditional Input-Output Approach (IOA), originally developed by Wassily Leontief [33], with a multiregional perspective, allowing the examination of interactions across various economic sectors and countries worldwide. Multiregional Input-Output Tables (MRIOTs) are employed to estimate the impact on the demand for goods and services produced in a particular country when investments are made in different regions or countries.

A technical coefficient matrix (representing relations between the various industrial sectors) and socioeconomic or environmental diagonalized vectors are used to quantify impacts on goods and services production, value-added creation, employment generation and CO_2 emissions.

The database from which both the MRIOT and the socioeconomic data have been used is the World Input Output Database (WIOD) [34]. The present study aggregates this MRIOT for the year 2014 to 8 regions (European Union, United States, Japan, China, Korea, Russia,

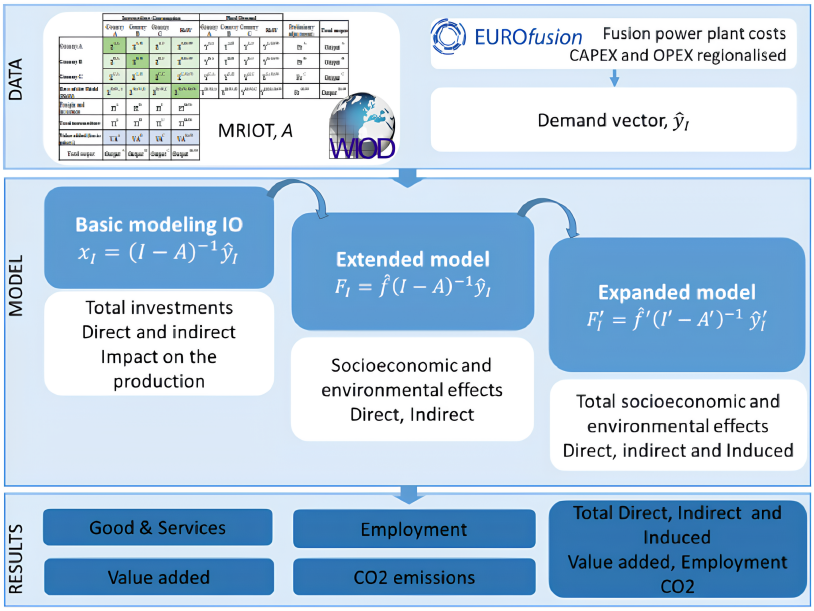

Figure 1.6. Flowchart of the process and methodological scheme at the basis of the EMRIO.

India and the Rest of the World).

Notably, the study focuses on various phases of the fusion power plant project, with particular emphasis on the investment phase, recognizing its pivotal role in influencing economic growth, employment patterns, and carbon footprint. The employed methodology aims to capture both direct and indirect effects and evaluates the potential advantages for countries involved in the fusion project.

The findings highlight that Europe and the United States stand out in terms of production and value-added benefits, with mining, construction, and business services experiencing significant positive effects (Figure 1.7 (a)).

Moreover, the analysis projects fusion power as an employment-intensive technology, estimating 133.6 FTE/MW[3] during the investment and operation phases (Figure 1.7 (b)). The European Union, China, and India emerge as the primary beneficiaries concerning employment generation. It is noteworthy that India and China's employment impact is more substantial during the operation and maintenance (O&M) stage.

Regarding the carbon footprint shown in Figure 1.7 (c), the study anticipates a reduction to 11.4 g_{CO2}/kWh, mainly originating in Europe, USA and Japan.

The methodology employed in this study has notable limitations in predicting the socioeconomic impacts of a fusion power plant. Firstly, Input-Output (IO) tables, which form the basis of the analysis, depict economic structures as they existed in 2014. Assuming the persistence of the same structures in future world economies may be unrealistic, rendering the analysis a counterfactual exercise focused on current impacts. Secondly, the extension vectors for socioeconomic and environmental factors reflect the present situation, while the employment or emissions intensity of sectors changes over time. Lastly, the level of sector aggregation may lead to insufficient description of the specific socioeconomic effects of certain materials and components. Despite these limitations, the simplicity of the model makes it a suitable approach for estimating sustainability impacts.

[3]Full-time equivalents per megawatt (FTE/MW) is a measure indicating the number of full-time workers needed to produce or operate one megawatt of energy.

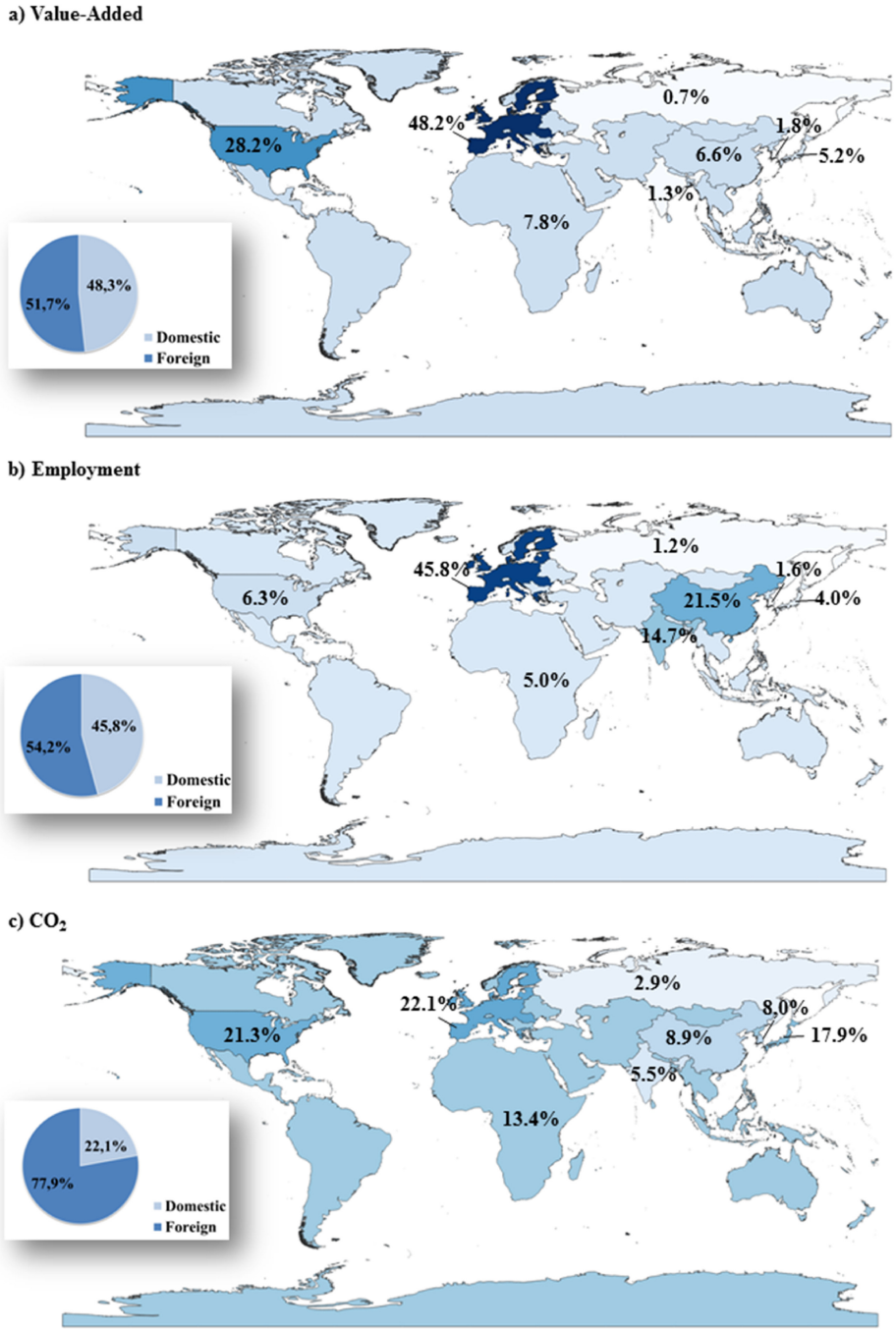

Figure 1.7. Regional participation in terms of value-added (a), FTE employment creation (b), and CO_2 emissions (c).

1.2 Fundamentals of Nuclear Fusion Theory

Nuclear fusion is the extraordinary process powering the Sun and stars as their primary energy source. It stands in stark contrast to its nuclear counterpart, fission. In a nutshell, while fission involves the division of heavy nuclei releasing energy, fusion commences with light elements, bringing them together to form heavier elements.

These two reactions, despite being inverse processes, are grounded in the concepts of "mass defect" and Binding Energy. According to nuclear particle experiments, the total mass of a nucleus is lower than the sum of the masses of its constituent nucleons (protons and neutrons). This means, that the total energy of a nucleus is less than the sum of the energies of its constituent nucleons, because of the mass–energy equivalence $E = mc^2$. Thus, the formation of a nucleus from a system of isolated protons and neutrons is an exothermic reaction and the energy emitted in this process, called Binding Energy (E_b), is equal to $\Delta m \cdot c^2$.

It is not only the amount of energy released in forming the nucleus, but also the energy required to break apart the nucleus.

This binding force is contingent on the number of nucleons, protons or neutrons, constituting the nucleus. The experimental quantity Binding Energy per Nucleon (BEN) or mean binding energy, expressed by the Eq. (1.2), where A is the mass number, provides valuable insights, as depicted in Figure 1.8, where nuclei with mass close to ^{56}Fe exhibit the highest BEN. Consequently, fusion of nuclei with mass numbers less than Fe and fission of those with mass numbers greater than Fe are exothermic processes.

$$\text{BEN} = \frac{E_b}{A} \tag{1.2}$$

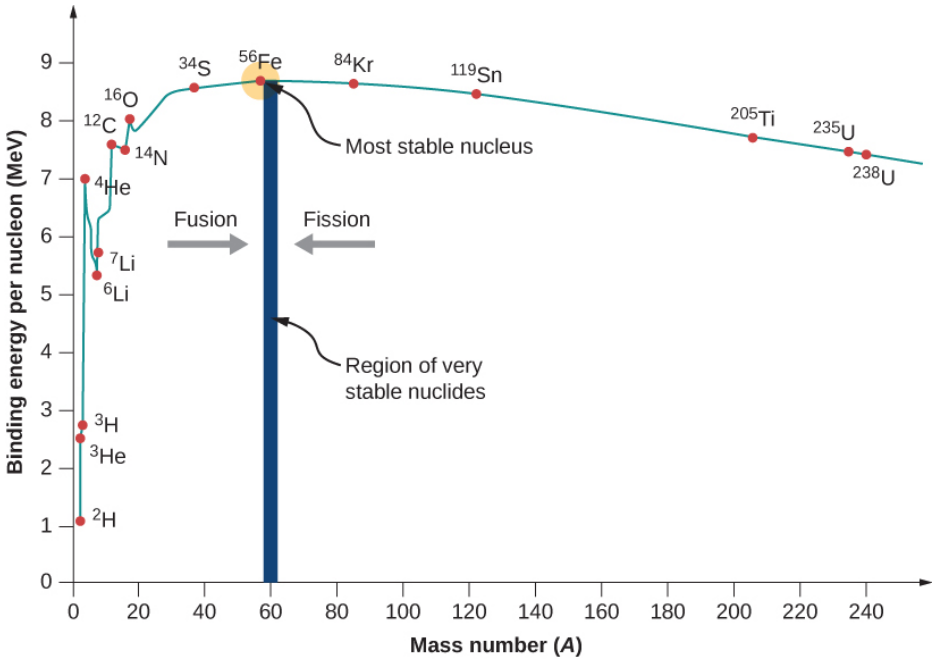

Figure 1.8. BEN vs A, the nuclear force that binds nucleons together within a nucleus. The chart also serves as a representation of the energy released during the transmutation of one element into another, with fission on the right side and fusion on the left. Comparing the two processes reveals that fusion transmutations release considerably more energy than fission.

In light atoms with few nucleons (e.g. hydrogen) the mean binding energy released to add another nucleon to the nucleus is very high. Notably, elements in the middle of the periodic table exhibit the highest binding energy. Considering the fission of Uranium-235 (^{235}U), commonly used as reagent, the process hinges on a chain reaction initiated by bombarding ^{235}U with neutrons, resulting in the release of energy. The mass defect, stemming from the mass-energy equivalence, is the driving force behind energy generation in nuclear fission. However, fission's drawbacks include its inherent danger due to the chain reaction and the radioactivity of its byproducts.

Conversely, nuclear fusion hinges on the combination of light nuclei atoms into a heavier nucleus atom. Notably, the fusion of two isotopes of hydrogen - deuterium (D or 2H) and tritium (T or 3H) - into Helium (He) is of particular interest. While Deuterium is abundant on Earth, Tritium is not stable, being radioactive with a half-life of 12.3 years. Fusion reactions release energy through a mass defect, where the combined mass of D and T is greater than the mass of the resulting products. The excess energy is predominantly carried away by the released neutron.

Achieving fusion poses the challenge of overcoming the inherent repulsion between positively charged protons or heavier nuclei. In celestial bodies like stars, this hurdle is surmountable due to the intense conditions at their cores, where gravitational forces counteract thermal expansion. In these extreme environments, electrons become detached from nuclei, turning a gas into a plasma, a state often identified as the fourth form of matter. Fusion plasmas provide the setting for the fusion of lightweight elements, resulting in the release of energy.

On Earth, replicating fusion in a laboratory necessitates meeting three essential conditions: exceptionally high temperatures; a sufficient density of plasma particles to enhance collision probabilities; adequate confinement time to contain the plasma, which tends to expand within a specified volume.

In the laboratory, achieving controlled thermonuclear fusion with a positive energy balance requires temperatures of 100 million degrees Celsius, about six times the Sun's internal temperature. During the 20th century, researchers identified the most efficient fusion reaction attainable in a laboratory setting (Figure 1.9). This reaction involves deuterium (D) and tritium (T).

The DT fusion reaction, expressed by Eq. (1.3), is particularly efficient at generating energy. Occurring at relatively low temperatures of approximately 100 million degrees Celsius, this reaction fuses deuterium and tritium to produce a helium nucleus and a neutron, releasing 17.6 MeV of energy. Of this, 3.5 MeV is carried by the helium nucleus and the remaining 14.1 MeV by the neutron.

$$\mathrm{D} + \mathrm{T} \rightarrow \mathrm{He}^4 + n \tag{1.3}$$

While alpha particles (helium nuclei) remain in the plasma, contributing to its heating, neutrons, being electrically neutral, release their energy elsewhere, hitting and activating structural materials. One method of utilizing the neutrons is their reaction with lithium, contained in the Lithium-Lead blanket in the reactor [35], to produce tritium. This is significant since tritium, unlike deuterium, is rare and decays in approximately 12 years.

In the pursuit of controlled thermonuclear fusion, a plasma must be heated to extremely high temperatures (around 100 million degrees Celsius) and confined within a limited space for a sufficient amount of time. This allows the energy released from fusion reactions to offset both the energy used to produce the plasma and the losses due to various phenomena. This translates into the Lawson criterion, establishing the conditions necessary for achieving

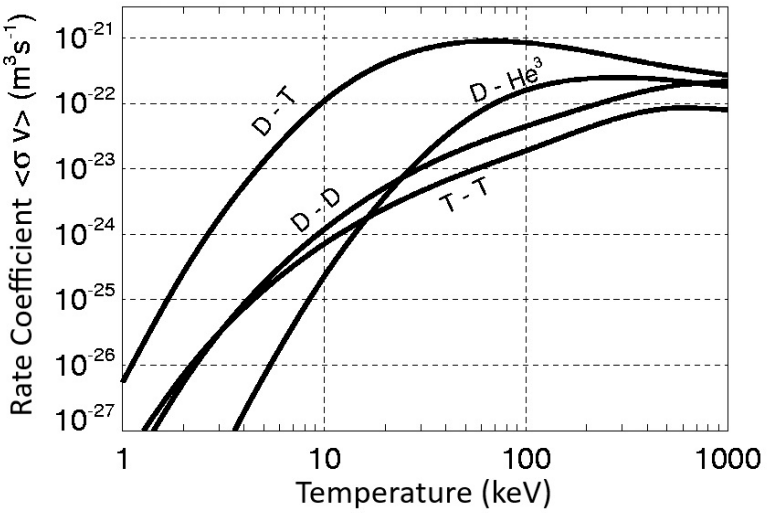

Figure 1.9. Reaction rate

a positive energy balance. This merit factor is given by the triple product of density (n), temperature (T), and plasma confinement time (τ_E), as expressed by Eq. (1.4) for the D-T reaction.

$$nT\tau_E \geq 3 \times 10^{21}\,\mathrm{keV} \cdot \mathrm{s} \cdot \mathrm{m}^3 \tag{1.4}$$

The fusion plasma must be confined within a limited space for a duration such that the energy released compensates for losses and the energy needed to produce the plasma itself. The Lawson criterion can also be expressed in terms of the power balance equation (Eq. (1.5)).

$$P_{\mathrm{ext}} + P_{\alpha} \geq P_{\mathrm{loss}} \tag{1.5}$$

Where:

- P_{ext} is the power that must be supplied externally to maintain the fuel in a plasma state, for example, by using additional heating.
- P_{α} is the energy from alpha particles, which impart their energy to the plasma through collisions.
- P_{loss} is the total power lost from the plasma due to various phenomena.

Achieving simultaneous high temperature, density, and confinement time presents a formidable task. If any of the three critical factors—temperature (T), density (n), or confinement time (τ_E) falls short, plasma confinement is compromised. Insufficient temperature prevents ions from overcoming the Coulomb barrier, reducing fusion reactions. Low density decreases the number of collisions, limiting energy production. A short confinement time causes energy to escape faster than it is generated, leading to plasma cooling. Thus, maintaining all three factors at optimal levels is essential to sustain the fusion process and achieve effective plasma confinement. As exposed in the next paragraph, two primary methods of plasma confinement have been developed and studied extensively: magnetic confinement and inertial confinement.

1.3 Technologies for Fusion Energy Production

Magnetic confinement involves the use of magnetic fields to trap and control the high-temperature plasma. Notable devices employing this approach include tokamaks and stellarators. Tokamaks, characterized by their toroidal shape as shown in Figure 1.10, create a magnetic field configuration that confines the plasma within a central region, preventing it from coming into contact with the reactor walls. Stellarators, with a more complex magnetic geometry (Figure 1.11), offer an alternative approach to maintaining plasma stability. While tokamaks rely on an internal plasma current to generate a poloidal field, stellarators utilize external helical coils. Due to this lack of a plasma current, stellarators inherently enable steady-state operation and exhibit reduced susceptibility to plasma instabilities.

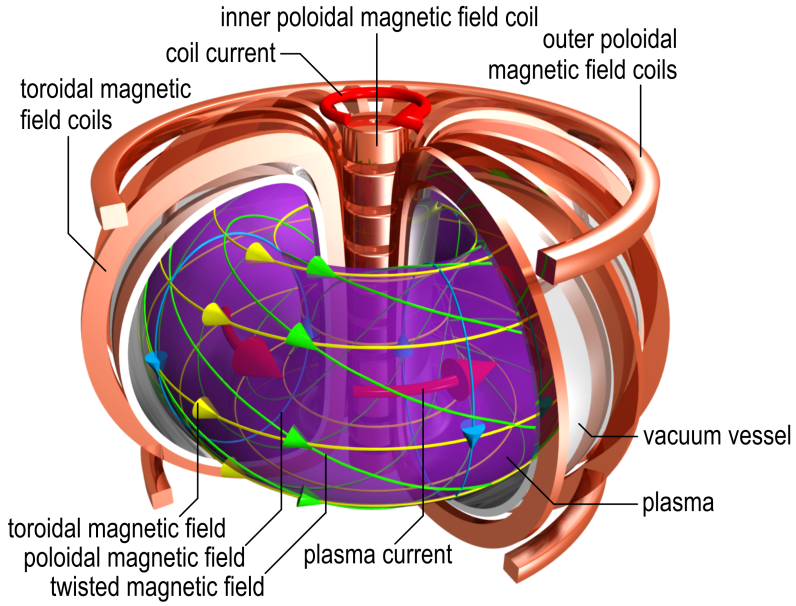

Figure 1.10. A schematic tokamak

Inertial confinement, on the other hand, relies on external forces to compress the plasma, thus achieving the required high temperatures and densities for fusion. This method often involves powerful laser systems or other intense energy sources directing energy onto a small pellet containing fusion fuel, causing implosion and heating. The rapid compression results in a brief but intense period of fusion reactions. Laser Inertial Fusion Energy (LIFE) [36] and National Ignition Facility (NIF) [37] are prominent examples of inertial confinement systems.

Both magnetic and inertial confinement approaches aim to meet the stringent Lawson criterion, ensuring that the power supplied to confine the plasma is sufficiently large to compensate for energy losses. Despite their distinct operational principles, these methods share the common goal of creating and sustaining the extreme conditions conducive to controlled fusion reactions.

1.3.1 Introduction to Tokamaks

Achieving effective plasma confinement is a crucial element in the operation of fusion reactors. In celestial bodies the gravitational field, generated by their mass, naturally confines plasma.

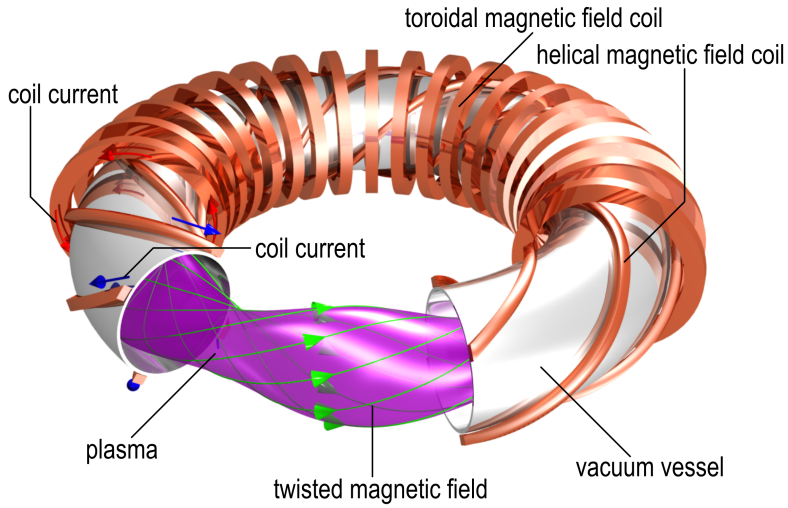

Figure 1.11. A schematic stellarator

On Earth, where such intense fields do not exist, fusion reactors must rely on alternative principles that have been studied over the years.

In particular, among the various devices designed for plasma confinement, tokamaks stand out a promising and advanced technology. Notably, they employ magnetic confinement in the configuration of a torus, shaping the plasma in a toroidal form. The magnetic trap generated within a tokamak serves to confine plasma particles effectively by spiraling them in a helical path, deflecting them away from the chamber walls.

Specifically, the resulting magnetic field is generated by a high direct current (in the order 10^4 kA) flowing into a complex system of large coils, most of which is made of superconductive windings operated at 4 K [38]. These coils are placed around the vacuum chamber containing the plasma. Their general structure, represented in Figure 1.10, consists of:

- Central Solenoid (CS): designed to produce an intense, highly time-varying magnetic field during the operational phase of the tokamak. This magnetic pulse serves multiple purposes, including initiating and sustaining the plasma current, contributing to the overall magnetic confinement, and controlling the behavior of the plasma.
- Toroidal Field Coils (TFCs): generating the primary toroidal magnetic field within the tokamak. This magnetic field configuration is crucial for confining the plasma in a toroidal shape, providing stability and facilitating controlled nuclear fusion reactions.
- Poloidal Field Coils (PFCs): generating the poloidal magnetic field in the tokamak. This additional magnetic field component, combined with the toroidal one, contributes to the overall magnetic confinement of the plasma. PFCs play a key role in shaping and controlling the plasma within the torus.

Other coil systems are incorporated directly into the vessel to ensure stable plasma operations. They include:

- Error Field Correction Coils (EFCCs) employed to mitigate deviations from the specified magnetic field referred to as Error Fields (EF) [39];

- In-vessel Divertor Coils (DVs) [40, 41], locally modifying the magnetic flux surfaces in the divertor region by adjusting the strike points to reduce wear on exposed surfaces and manage heat. Additionally, they assist in controlling alternative magnetic configurations and transitions between different plasma states;

- Vertical stability coils, which provide rapid vertical plasma stabilization, and the Edge Localized Mode (ELM) coils, that control plasma instabilities caused by large current and pressure gradients [42, 43].

It may also be noted that this list is not exhaustive.

While the CS acts like the primary circuit of a transformer, the plasma torus is viewed as the secondary circuit, with a resultant toroidal plasma current generating a poloidal magnetic field. To prevent plasma expansion, stabilizing coils introduce a vertical magnetic field. The complexity of this system serves the primary purpose of trapping particles to achieve nuclear fusion. The motion of charged particles along the magnetic field follows the Lorentz law [44], with only some particles trapped due to the variation of the magnetic field, resulting in a magnetic mirror effect[4]. The fraction of trapped particles is determined by the tokamak's aspect ratio, the geometric parameter used in describing the shape of a tokamak. Specifically, the aspect ratio A (defined by the Eq. (1.6)) refers to the ratio between the major radius R of the tokamak, measured from the center of the torus to the center of the toroidal tube, and the minor radius a representing the distance from the center of the torus to the outer edge of the toroidal tube.

$$A = \frac{R}{a} \tag{1.6}$$

In general, a tokamak with a smaller aspect ratio (closer to 1) has a more "pancake" shape, while a larger aspect ratio indicates a more "tubular" shape.

However, this confinement solution poses highly complex technological challenges, particularly related to the temperatures that vary, within a few meters, from hundred million degrees Celsius (required for the plasma) to temperatures near absolute zero (necessary for the operation of superconducting magnets surrounding the plasma).

Figure 1.12 shows the fundamental components of a tokamak core, highlighted in different colors. Each component in a tokamak reactor has a unique and vital role, working synergistically to achieve and sustain controlled nuclear fusion reactions.

The vacuum vessel (in yellow) is a hermetically sealed steel chamber that not only holds the fusion reactions but also serves as a primary confinement barrier for radioactivity. The vessel provides support for in-vessel components and a pathway for cooling water used during operation.

Enclosing the vacuum vessel and magnet systems is the cryostat (green), a large vacuum chamber providing the required ultra-cool environment. This chamber facilitates maintenance and interfaces with cooling systems, magnet feeders, additional heating, and diagnostics.

The Blanket (red), a modular coating covering the inner walls of the vacuum vessel, is crucial for protecting the steel structure and superconducting toroidal magnets from fusion heat and high-energy neutrons. It absorbs kinetic energy from neutrons, transforms it into heat, and uses cooling water for heat removal. The Blanket also undergoes Tritium breeding, a key element for the reactor's future development. The Tritium Breeding Blanket employs lithium to generate Tritium, an essential fuel for fusion reactions. Lithium-6 and Lithium-7

[4]While some particles are trapped, others follow different orbits, and the proportion of trapped particles can affect the overall stability and confinement of the plasma.

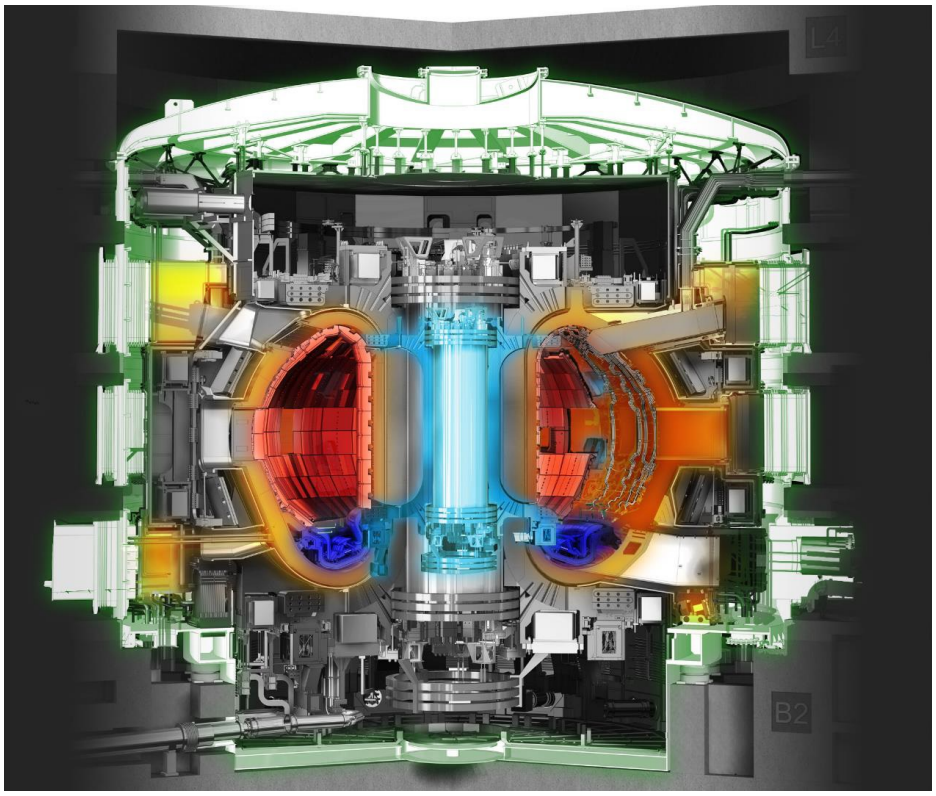

Figure 1.12. Main components of ITER tokamak chamber.

isotopes are particularly significant, with Lithium-6 being more useful for Tritium breeding. This process represents a cornerstone for the closed cycle of Tritium in future fusion reactors.

Finally, the Divertor (blue) manages a significant portion of the plasma exhaust. Its role includes reducing impurities, removing alpha particle power by heat exchange, and eliminating helium ash resulting from fusion reactions. Designing the divertor is a complex task due to its direct contact with the plasma and potential erosion from incoming impurities.

The intricate interplay of these components ensures the reactor's functionality, safety, and the progression of fusion research.

1.3.2 Existing Tokamaks

Although not an exhaustive list, the following paragraph aims to identify among existing tokamaks those that share common design features. A brief overview of JT-60SA (Japan), FTU (Italy), JET (UK), ITER (France), DEMO (TBD), and DTT (Italy) is provided.

- JT-60SA [45] is an international nuclear fusion experimental reactor located in Naka, Japan, resulting from the collaboration between Europe and Japan as part of the Broader Approach Agreement [46]. The acronym stands for "JT-60 Super Advanced", reflecting its use of superconducting coils for advanced plasma operations. The primary mission of JT-60SA is to support ITER operations through complementary research and development, aiming at optimizing post-ITER fusion power plant operation. Key research targets include operational regime development for ITER and DEMO, Magneto Hydro Dynamic (MHD) stability studies[5], confinement and transport studies, high-

[5]MHD is a branch of fluid dynamics that studies the behavior of electrically conducting fluids, such as

energy particle studies, pedestal studies[6] and studies on the Scrape-Off Layer (SOL), Divertor, and Plasma-Material Interaction.

JT-60SA uses powerful superconducting coils cooled to approximately -269 °C (absolute temperature approximately 4K) to confine the plasma.

The magnet system consists of toroidal field coils, a central solenoid, equilibrium field coils, and other components. The vacuum vessel, thermal shield, and in-vessel components, including divertor cassettes and cryopanels, are crucial for plasma containment and control. The cryostat, magnet shared components, and auxiliary plants for heating, power supply, cryogenics, cooling, and control contribute to the overall functionality of JT-60SA.

Marking a pivotal milestone in fusion research, JT-60SA successfully achieved its first plasma on October 23, 2023, solidifying its position as the world's largest operational superconducting tokamak.

- Joint European Torus (JET) [47] is an experimental tokamak located in Culham, UK. It was the largest operational tokamak in the world until October 23, 2023, when it was overtaken by JT-60SA. However, JET remains the largest operational tokamak capable of using tritium.

  JET has played an important role in advancing nuclear fusion research. In 1997 it reached a Q ratio of 0.67, marking the first time that fusion has produced more energy than was needed to start it. JET has also contributed to the development of new fusion technologies, such as neutral beam heating and MHD instability control. Currently in its decommissioning phase, JET is expected to cease operations in 2024. Despite its impending closure, JET's legacy continues to shape the future of fusion research. Its pioneering work has paved the way for next-generation fusion facilities like ITER, DEMO, and STEP.

  Recognizing the need for robust electronics in future fusion environments, JET is conducting crucial experiments to test electronics in fusion environments, representing a vital step in developing shielding for critical and safety electronics against neutrons in future fusion facilities. These experiments aim to understand how electronics respond to the neutron-rich environment produced during fusion, particularly in terms of Single Event Effects (SEEs), which are malfunctions or failures caused by neutron interactions. The findings from JET's experiments will inform the design and protection of electronic components for future fusion machines, ensuring their reliability in the harsh neutron environment of tokamaks like ITER and DEMO. Additionally, the research findings hold broader implications for industries that require electronics to operate in extreme environments, such as the nuclear, automotive, avionics, and space sectors.

- Frascati Tokamak Upgrade (FTU) [48], operational since 1990, is a compact, high-magnetic-field tokamak designed to study plasma heating, current drive, energy and particle confinement, as well as plasma-wall interaction. It is located in the ENEA Research Center in Frascati, which has been a pioneering force in nuclear fusion research since the late 1950s, particularly through the construction and operation of magnetic confinement tokamak experiments, including the Frascati Tokamak (FT) and Frascati

plasmas, in the presence of magnetic fields. MHD instabilities can disrupt the plasma confinement, leading to a loss of energy and potential damage to the device's components. Studying MHD stability is, therefore, critical for developing and maintaining stable and efficient fusion plasma conditions.

[6]The pedestal is a high-pressure and high-density region located at the edge of the plasma.

Tokamak Upgrade (FTU). These experiments have yielded internationally significant results and influenced strategic decisions for the future.

Both experiments have contributed significantly to exploring heating capabilities, especially with Radio Frequency (RF) emitters. FTU, in particular, with its higher power heating systems, has achieved remarkable temperatures and record-breaking densities, positioning it at the forefront of global scientific discussions.

Over the years, FTU has achieved other notable milestones, such as the successful stabilization of post-disruption runaway electron beams and the testing of liquid tin as a resilient plasma-facing component material. The installation of a vertical controller proved effective in stabilizing vertically elongated plasmas, achieving record elongation levels. Dust mobilization studies highlighted the impact of magnetic dust in the FTU vessel, influencing tokamak operations [49].

Currently the FTU machine is in its decommissioning phase, as part of the activities aimed at making available the environments that will be used for the DTT infrastructure.

- The Divertor Tokamak Test facility (DTT) [50], currently under construction in Frascati, Italy, represents a crucial venture in advancing fusion research. DTT is a tokamak featuring a 6 T on-axis maximum toroidal magnetic field, with a plasma current capacity of up to 5.5 MA in pulses lasting up to 100 s. The D-shaped vacuum chamber, with a major radius (R) of 2.19 meter, minor radius (a) of 0.70 meter, and average triangularity of 0.3, is designed for flexibility in accommodating various divertor configurations.

  The primary focus of DTT lies in addressing the challenges associated with the heat-exhaust system, particularly the divertor. The divertor plays a crucial role in handling the heat generated by fusion reactions, especially alpha particles, and preventing damage to the plasma-facing components. DTT aims to demonstrate innovative solutions for the divertor, exploring advanced magnetic configurations and novel materials such as liquid metals. These solutions are imperative as the standard divertor components currently withstand heat fluxes up to $20\,\mathrm{MW/m^2}$ for a limited time, while the anticipated heat flux in fusion power plants could reach levels comparable to the surface of the Sun, around $60\,\mathrm{MW/m^2}$.

  DTT's design emphasizes flexibility to accommodate different divertor configurations, and its 45 MW auxiliary heating power, comprising ion and electron cyclotron resonance heating and negative ion beams, aligns with the requirements of ITER and DEMO. The superconducting systems, including Toroidal, Poloidal Field, and Central Solenoid, enable DTT to generate a magnetic field akin to ITER and DEMO.

  The divertor system in DTT is a core element, featuring 54 modules compatible with various scenarios, including the reference single null scenario with positive triangularity and alternative scenarios for DEMO. The DTT diagnostic system, comprising about 80 techniques, ensures precise measurements in core, edge, and divertor areas, essential for machine protection, plasma control, and supporting the scientific program.

  Additionally, DTT incorporates a remote handling system for preventive maintenance actions, showcasing its comprehensive approach to facility management. The DTT Research Plan outlines strategic directions, covering scientific exploitation, divertor and SOL physics, plasma scenarios and modeling, heating, current drive and fueling, MHD and fast particles theory, and fusion technology developments. The plan has been evolving over the years and involves contributions from EUROfusion scientists.

As DTT progresses, it will operate initially at reduced plasma current and with half of the external additional power, allowing for testing different divertor modules. In the long term, DTT aims to achieve nominal heating, providing valuable insights into effective solutions for DEMO and other tokamak divertors. This ambitious project is a testament to the collaborative efforts and dedication of the fusion research community, marking a significant stride towards the realization of fusion energy.

- ITER [51] represents one of the most ambitious energy projects globally. Situated in southern France, this collaborative effort involves 35 nations collaborating to construct the world's largest tokamak.

  At the heart of ITER's mission is the exploration and demonstration of burning plasmas where the energy from fusion reactions sustains the plasma's temperature, potentially reducing or eliminating the need for external heating. The project also aims to test and integrate essential technologies for a fusion reactor, such as superconducting magnets, remote maintenance, and plasma power exhaust systems. Additionally, ITER seeks to validate tritium breeding module concepts for future reactor self-sufficiency.

  The ITER collaboration involves seven members: China, the European Union, India, Japan, Korea, Russia, and the United States. These nations are committed to a long-term collaboration to construct and operate the ITER experimental device, paving the way for the development of a demonstration fusion reactor.

  The objectives of ITER include achieving a deuterium-tritium plasma sustained by internal fusion heating, generating 500 MW of fusion power in its plasma, demonstrating integrated operation technologies for a fusion power plant, testing tritium breeding, and showcasing the safety characteristics of a fusion device. The construction of ITER involves a complex assembly of components delivered by the participating nations. Europe bears most of the construction costs, with the remainder shared equally among the other members. The collaboration extends beyond monetary contributions, as the members provide completed components, systems, or buildings, fostering a truly global effort.

  The timeline of the project spans from the decision to site it in France in 2005 to the ongoing construction phase, with the ITER Council considering an updated project baseline to address challenges and maintain progress.

Chapter 2

Nuclear Fusion Power Plants

Nuclear fusion holds the promise of a sustainable and abundant energy source, capable of revolutionizing the global energy landscape. However, harnessing the power of fusion demands a meticulous approach, adhering to stringent requirements that encompass design, operation, and safety. This chapter delves into these essential requirements that draw inspiration from established practices in nuclear fission and elucidates the distinct features of nuclear fusion, highlighting the paramount importance of safety considerations.

The exploration begins with an overview of the main systems of a nuclear fusion power plant, providing a comprehensive examination of the critical components that form the backbone of these energy facilities.

Subsequently, the chapter navigates through the principles of facility connection to the grid, offering a detailed insight into the integration of NFPPs with national and European power grids. By examining segments of the European Network Codes and the Italian Grid Code, the overview underscores the interconnectedness of nuclear fusion with broader energy infrastructure.

In the pursuit of safe and reliable nuclear fusion, the chapter culminates in an exploration of the fundamental safety guidelines for the facility. A compilation of standards, including those defined by the IEEE, outlines the stringent measures and protocols necessary to ensure the secure operation of NFPPs.

Through this multifaceted exploration, the chapter aims to provide a holistic understanding of the requirements that govern nuclear fusion power plants, shedding light on both the borrowed wisdom from nuclear fission and the distinctive facets that define the safety paradigm in the realm of fusion energy.

2.1 Main Systems of a Nuclear Fusion Power Plant

At the heart of every NFPP lies a complex network of interconnected systems, each playing a crucial role in the delicate process of generating fusion energy. To fully comprehend the unique challenges and opportunities posed by nuclear fusion, a comprehensive understanding of these critical components is essential.

- Plasma Confinement System: The cornerstone of a NFPP is the plasma confinement system [52] [38] which, employing powerful magnets, creates a controlled environment where the plasma can reach the extreme temperatures and pressures required for fusion to occur.

- Plasma Heating System: To initiate and sustain fusion, the plasma must be heated to temperatures exceeding 100 million degrees Celsius. This formidable task is entrusted to the plasma heating system [53], which utilizes various techniques, such as radio waves or neutral beam injection, to inject energy into the plasma.
- Tritium Breeding System: Tritium, one of the key isotopes for fusion reactions, is a rare and expensive resource. To address this challenge, NFPPs incorporate tritium breeding systems, utilizing neutrons from the fusion process to produce tritium from lithium.
- Tritium Handling System: Tritium, a radioactive isotope, demands careful handling to ensure safety and prevent environmental contamination. The tritium handling system [54] meticulously manages the tritium cycle within the NFPP, encompassing its production, storage, and purification.
- Power Conversion System: The energy released from fusion reactions is harnessed by the power conversion system, transforming the thermal energy into electricity. This system typically employs a heat exchanger to transfer heat from the plasma to a secondary fluid, which then drives a turbine-generator to produce electricity.

2.2 Principles for Grid Integration of NFPP

The seamless integration of NFPPs into existing power grids is crucial for their successful deployment. This paragraph delves into the principles of plant network connection, examining the intricate interplay between NFPPs and the European and Italian power grids.

The European Network Codes [55] are a set of rules and guidelines developed by the European Network of Transmission System Operators for Electricity (ENTSO-E), with guidance from the Agency for the Cooperation of Energy Regulators (ACER), and adopted by the European Commission. These codes aim to harmonize electricity grid connection regime, as well as efficient and secure operations, and to improve the functioning of the European electricity market. They are fundamental to achieve the European Union's energy objectives, including a 55% reduction in greenhouse gas emissions compared to 1990 levels, a 32% share of renewable energy consumption, and a 32.5% decrease in energy consumption compared to the business-as-usual scenario[1].

The network codes play a crucial role in achieving ambitious goals for a secure, competitive, and low-carbon European electricity sector and internal energy market. They provide a legal framework by defining a common 'code of conduct' for sector participants, harmonizing practices, and facilitating market integration. As shown in Table 2.1, the codes encompass four "families", each serving a specific purpose in the European electricity sector: Market codes for competition and resource optimization, Connection codes for linking actors to the grid, Operational codes for grid operation security, and the newly introduced Cybersecurity Code, setting a European standard for ensuring the cybersecurity of cross-border electricity flows. Having concluded the development phase, the focus is now on implementation, making the codes binding EU law. Successful implementation involves stakeholder consultation, regulatory approval, and coordination at national and European levels, requiring the active involvement of the entire electricity community.

[1] Baseline scenario that examines the consequences of continuing current trends in population, economy, technology and human behaviour.

Table 2.1. Network Code Families.

Family	Objective	Key Elements
Market Codes	Foster competition and optimize resource utilization in the market.	Rules and guidelines promoting fair competition, market transparency, and efficient resource allocation.
Connection Codes	Establish connections between various actors and the electricity grid.	Standards and protocols for linking participants to the grid, ensuring seamless and reliable interactions.
Operational Codes	Enhance grid operation security.	Protocols and procedures for ensuring the secure and stable operation of the electricity grid.
Cybersecurity Code	Set a European standard for ensuring the cybersecurity of cross-border electricity flows.	Measures and guidelines to protect the integrity and security of the electric grid against cyber threats.

Regarding the second "family", three network codes on grid connection have been developed:

- The Network Code on Requirements for Grid Connection of Generators, also known as Network Code Requirements for Generators (NC RfG) [56], established by the Commission Regulation (EU) 2016/631. This regulation sets out the technical requirements for the connection of generators to the grid, aiming to ensure the secure and efficient operation of the European electricity system.
- The Network Code on Demand Connection (DCC Regulation) [57], established by Commission Regulation (EU) 2016/1388. It sets up harmonised requirements for connecting large renewable energy production plants as well as demand response facilities.
- The Network Code on Requirements for Grid Connection of High Voltage Direct Current (HVDC) Systems (HVDC Regulation) [58], established by Commission Regulation (EU) 2016/1447. It covers the definition of harmonised standards for Direct current (DC) connections.

In December 2023, ACER proposed amendments to the first two grid connection codes to the European Commission to support the EU power grid in adapting to emerging developments such as e-mobility, storage, and energy communities. These codes ensure that future NFPPs seamlessly integrate into the European power system, contributing to a stable and secure energy supply.

National-level implementation of this regulation involves each EU member State incorporating its provisions into their national legislation and ensuring compliance by relevant stakeholders such as grid operators, generators, and regulators. To support the implementation at the national level, ENTSO-E has drafted a set of non-binding implementation guidance documents, highlighting the effect on specific technologies, the link with local

network characteristics, and the need for coordination between network operators and grid users.

The development of electricity transmission infrastructure across Europe has been influenced by distinct national factors, including geographic size, topographical features, and economic considerations. Furthermore, the extent of interconnection between European countries varies significantly, reflecting individual energy policies and infrastructure investments. Therefore, the implementation of the three network codes on connection, aims at harmonizing cross-border electricity transmission practices, necessitates a balanced approach that incorporates national-level parameters and pan-European guidelines.

With particular reference to the NC RfG, the provision of this network code generally applies to new Power Generating Modules (PGMs) that will have a significant impact on the system operation, notably PGMs recognized as "significant grid users"[2] by Article 5 of the NC RfG.

Depending on their technical requirements, the PGM units are divided into four types with increasing requirements from one category to another, as summarized in Table 2.2. Requirements on the voltage at the connection point and on maximum capacity of the plant are also indicated in Table 2.3).

In consideration of the diversity of generation structures across the individual countries covered by this network code, the capacity power thresholds have been differentiated and defined for each synchronous area individually, as illustrated in Figure 2.1. As part of the national implementation, these capacity thresholds are intended to be determined in accordance with Article 5, Paragraph 3 of the NC RfG, aligning with the needs of the National Power System (NPS) by the respective Transmission System Operator (TSO). Specifically, the TSO is responsible for formulating the general requirements and capacity thresholds applicable to generating modules of types B, C, and D. Simultaneously, the TSO collaborates with the Distribution System Operator (DSO) in this endeavor, ensuring the transparency of the entire process. This responsibility falls under the operator's purview concerning the safety of the system, as outlined in Article 7, Paragraph 3. These regulations and thresholds must be developed within a two-year timeframe from the entry into force of the NC RfG. Additionally, they are subject to approval by the Energy Regulatory Office, as specified in Article 7 - Paragraph 4.

In addition, the requirements are further categorized taking into account the grid connection of the generating module as follows:

- Generating modules connected synchronously to the grid, referred to as Synchronous Power Generating Modules (SY PGMs), which is typical for conventional power plants and combined heat and power plants.
- Non-synchronous, using power electronic converter systems, commonly found in wind and solar energy-based Renewable Energy Source (RES) and known as Power Park Modules (PPMs).

2.3 Safety Guidelines for Nuclear Fusion Facilities

Despite ongoing development of fusion power plant concepts since the 1950s, a specific regulatory framework dedicated to the safety of these facilities remains absent. Consequently,

[2]Pre-existing grid users and new grid users which are deemed significant on the basis of their impact on the cross border system performance via influence on the control area's security of supply, including provision of ancillary services.

Synchronous Area	Max. capacity for type B	Max. capacity for type C	Max. capacity for type D
Continental Europe	1 MW	50 MW	75 MW
Nordic	1 MW	50 MW	75 MW
United Kingdom	1.5 MW	10 MW	30 MW
Ireland	0.1 MW	5 MW	10 MW
Baltic	0.5 MW	10 MW	15 MW
	and	**and**	**or**
Voltage	< 110 kV	< 110 kV	≥ 110 kV

Figure 2.1. Maximum Capacities and Voltage Levels for Synchronous Areas.

current safety approaches draw on established concepts from the fission power world. A set of generic recommendations developed at an international level are used as reference, comprising the International Atomic Energy Agency (IAEA) guidelines which propose an approach for any nuclear facility (including, notably, the defence-in-depth and As Low As Reasonably Achievable (ALARA) concepts [59]). Several European studies demonstrate the continuous progress in fusion safety, including the Safety and Environmental Assessment of Fusion Power (SEAFP) [60] and the Safety and Environmental Assessment of Fusion Power – Long Term Programme (SEAL) [61]. These studies, along with the Power Plant Conceptual Study (PPCS) [62] served as the foundation for fusion reactor design while additionally identifying key safety factors and blanket types. Moreover, the safety analysis conducted during the licensing of ITER documented in the Rapport Préliminaire de Sûreté (Preliminary Safety Report - RPrS) [63], provides a valuable reference point, currently representing the most comprehensive overview of a fusion safety concept. As a type of nuclear energy, fusion shares some safety concerns with fission (however at a different level of severity), primarily regarding nuclear accidents with environmental release of radioactive materials and radioactive waste management. Notably, the most significant potential risks in fusion accidents involve the atmospheric release of:

- **Tritium:** This release is characterized by extremely low probability even in large quantities.
- **Activated Materials:** These primarily originate from components within the vacuum vessel, including the plasma-facing components and blanket segments. Two main accident scenarios with potential release of activated materials are:
  - **Plasma Disruptions:** This occurs when the plasma loses stability and releases its energy onto the chamber walls, potentially causing localized vaporization and melting, leading to chamber rupture and air/vapor ingress (Loss Of Vacuum Accident - LOVA).
  - **Primary Coolant System Accident:** A complete or partial failure of the cooling system leads to immediate reactor shutdown. However, the afterheat generated in activated structures can still raise the temperature of certain components to melting point (Loss Of Cooling Accident - LOCA).

Both scenarios can lead to chemical interactions between melted/vaporized materials, potentially producing radioactive vapors. Additionally, activated corrosion products present in the coolant may be vaporized and released.

While acknowledging the relatively low, yet non-negligible, safety concerns in fusion machines, it is crucial to address these challenges before construction begins. The defense-in-depth approach is a cornerstone of nuclear power plant safety. This principle emphasizes multiple layers of protection ("barriers") organized into a tiered approach, focusing on prevention, control, mitigation and consequence limitation. The IAEA specifies five levels of defense [64], grouped in Table 2.5.

The ALARA principle is significant as well, not just for demonstrating compliance with specified objectives but also for implementing practical measures to minimize radiation doses to workers in both normal and abnormal scenarios.

2.3.1 Designing Safety: Electrical Systems in Nuclear Power Plants

A fusion power plant has different parts that play a crucial role in maintaining safety. These crucial elements (Structures, Systems and Components (SSCs)) are called Safety Important Component (SIC). SICs are categorized based on their specific functions related to preventing or mitigating potential incidents or accidents. They fall into different categories based on the following criteria:

- Criterion A SICs: These are components whose failure could directly trigger an incident or accident, potentially leading to exposure or contamination risks.
- Criterion B SICs: These components are essential for limiting the consequences of an incident or accident that could otherwise lead to significant exposure or contamination risks.
- Criterion C SICs: These components are crucial for ensuring the proper functioning of other SICs.

Thus, two classes of SIC are defined:

- SIC-1: These are essential for bringing and maintaining the plant in a safe status.
- SIC-2: These are specifically used to prevent, detect or mitigate incidents or accidents

Components that are not considered SIC are categorized as "non-SIC". However, some non-SIC components may still be "Safety Relevant (SR)" meaning that they can still have an impact on safety and require specific attention during design and operation.

To ensure the reliable operation of critical components, power sources are categorized into distinct Voltage Classes based on their ability to tolerate interruptions, as summarized in Table 2.6. As depicted in Figure 2.2, higher Voltage Classes (I and II) offer shorter maximum interruption times but are typically more expensive per kW. Conversely, lower Voltage Classes (III and IV) allow for longer interruptions but are more cost-effective. This classification system not only safeguards safety-critical systems but also optimizes resource allocation by matching power supply characteristics to the specific needs of the loads.

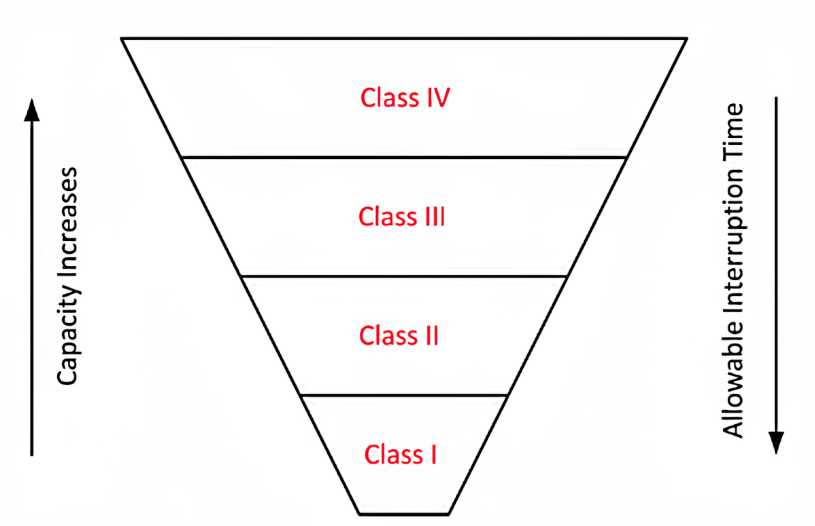

Figure 2.2. Relationship between System Capacity and Allowable Interruption Time.

Table 2.2. Plant Categories and Requirements

Category	Requirements
A **Small-scale Plants**	– Remain connected to the grid within specified frequency ranges. – Provide over-frequency response for grid stability. – Automatic reconnection to the grid without limits on injected power.

B
Medium-scale Plants: Type A Requirements +
	– Data/Information Exchange:
	  – Exchange relevant data and information with the grid operator.
	  – Provide visibility of generation plants and their operating status.
	– Reconnection to the Grid:
	  – Reconnect under certain injected power conditions.
	  – Insensitivity to voltage variations.
	  – Partial contribution to voltage regulation.

C
Large-scale Plants: Type A and B Requirements +
	– Advanced Frequency Stability:
	  – Implement advanced frequency stability measures (frequency restoration, frequency/power response, etc.).
	– Electrical System Management:
	  – Implement transient recording.
	  – Include protections for the electrical system.
	– Voltage Regulation:
	  – Contribute to local voltage regulation.
	  – Ensure local voltage stability.

D **Extra-large Scale Plants: Type A, B, and C Requirements +**	– Meet all voltage regulation and stability requirements for the electrical grid.

Table 2.3. Categories of PGMs based on Voltage Level at the connection point and maximum capacity.

Category	Voltage Level [kV]	Maximum Capacity [kW]
Type A	< 110	> 0.8
Type B	< 110	> 1000
Type C	< 110	$> 50\,000$
Type D	> 110	$> 75\,000$

Table 2.4. Definition of the Voltage Level of Connection

Category	Power Rating of the Facility	Nominal Voltage Level
Generation	6 – 10 MW	MV ÷ 150 kV
	10 – 100 MW	120 – 150 kV
	100 – 250 MW	120 – 150 kV
	200 – 350 MW	220 – 380 kV
	200 – 350 MW	220 – 380 kV
	Structured in more than one generation sets	220 – 380 kV
	> 350 MW	380 kV
Demand	< 10 MW	MV ÷ 150 kV
	10 – 20 MW	60 ÷ 150 kV
	20 – 50 MW	120 ÷ 150 kV
	30 – 100 MW	120 ÷ 150 kV
	> 100 MW	220 – 380 kV

Table 2.5. Defence in depth principles.

Level	Principles
1st level Prevention	Quality in design and fabrication Prevention of non-conformity
2nd level Surveillance detection and control	Quality of operation keeping the facility within authorized limits
3rd level Safety systems	Implantation of means to limit the effects of accidents
4th level Accident management and containment protection	Prevention of deterioration of accidental conditions
5th level Response outside the site	Limitation of consequences

Table 2.6. Classification of power sources.

Class of Power	System Load Characteristics and Description
Class I	Power can never be interrupted under postulated conditions. Supplies the most critical and safety-related systems. It is a DC power source with three independent distribution channels, each backed by battery banks to ensure uninterrupted power. Failure of Class I power may trigger a reactor shutdown.
Class II	Power can be interrupted up to 4 milliseconds. Supports systems that can tolerate power interruptions on the order of milliseconds. Power is typically supplied from Class I through inverters, ensuring continuous operation of critical instrumentation and control systems.
Class III	Power can be interrupted up to 5 minutes. Maintains essential functions like fuel cooling when the reactor is in a shutdown state and Class IV power is unavailable. Standby generators* are used to restore Class III power quickly in case of an outage.
Class IV	Power can be interrupted indefinitely. Supplies non-critical systems that can tolerate long-term outages. Power is sourced either from the main generator or the grid, ensuring minimal impact on safety-critical operations.

* A standby generator is a diesel-powered generator that provides backup power to critical systems when the primary Class IV power source fails. It starts automatically within 30 seconds after a loss of Class IV power, and it can run continuously for extended periods.

Chapter 3

Power System Studies for Fusion Facilities

Power system studies play a crucial role in ensuring the safe and efficient operation of a fusion facility's electrical infrastructure. Developing an accurate power system model for simulation studies not only enhances the site's safety, by facilitating the identification and mitigation of potential hazards within the electrical system, but also optimizes costs by maximizing existing infrastructure and providing confidence for investment plans in future upgrades or expansions.

The foundation of a comprehensive power system study lies in the data collected and incorporated into the Electrical Load List (ELL) This document serves as a "living record", continuously updated with the main information of the electrical loads, such as rated power, power factor and duty cycle, evolving as the knowledge of the system increases.

This chapter presents the network studies conducted for the two case studies analyzed throughout my PhD research, aiming to gain a deeper understanding of the overall functioning of the power system of a nuclear fusion facility and identifying potential improvements within the electrical infrastructures under consideration.

Specifically, these studies focused on power system analyses for Divertor Tokamak Test (DTT) and the DEMO projects. In the case of DTT, the focus was on both the Pulsed Power Electrical Network (PPEN) and Steady-State Electrical Network (SSEN) (see paragraph 3.2). In contrast, for DEMO the analysis was concentrated solely on the on the steady-state loads of the Medium and Low Voltage Network (MLVN) (see paragraph 3.3), as the University of Padova is responsible for simulating the pulsed loads. PowerFactory software was employed to model the electrical infrastructure of both DTT and DEMO, including substations, switchgears and feeder lines, with the purpose to obtain the performance of the system in different operating conditions. The studies helped quantify the impact of additional loads, evaluate network modifications, and assess the validity of the initial assumptions regarding equipment sizing.

The overall work is divided into three major steps: deterministic simulations, probabilistic simulations, and sensitivity analyses.

3.1 Methodology and Mathematical Formulations

The methodology employed in the study of power systems for fusion facilities involve a comprehensive approach that includes the following steps:

- System Characterization: Detailed analysis of the electrical distribution network, including load profiles, generation capabilities, and grid interconnections.
- Model Development: Creating accurate models for different components of the power system, such as transformers, transmission lines, and power supplies.
- Simulation Techniques: Utilizing deterministic and probabilistic power flow simulations to analyze the behavior of the power system under various conditions and uncertainties.
- Sensitivity Analysis: Identifying critical uncertainties and their impacts on the power system.

As regards the first point, central to the analysis of the electrical distribution network is the characterization of the electrical loads to ensure that the power distribution system can meet the demands of the facility under various operating conditions. The ELL is fundamental to this characterization, providing a detailed inventory of all the electrical loads within the facility, and categorizing them based on their specific requirements (load type, rated power, location), operational characteristics (voltage level, utilization and coincidence factors), and the criticality of their functions (voltage class, safety class and redundancy). This allows for the proper allocation of power, the sizing of electrical components, and the implementation of effective control strategies.

In a NFPP, the different nature of the electrical loads that require dedicated and separate sections of the internal distribution network has the greatest impact on the system's specifications. Based on their power profiles, these loads are defined as follows:

- Steady-state loads: Exhibiting a constant or quasi-constant profile with slow variations, such as lighting systems and heating elements.
- Pulsed loads: Characterized by intermittent operation with high peak currents, often comparable to the equipment rating. These rapid variations can have significant impacts on the electrical network, potentially causing deep voltage drops and even load disconnections, such as plasma control systems.

Other than power profiles, loads can also be classified on the basis of other characteristics relevant for system design, e.g., based operational continuity, into [65]:

- Ordinary loads (OL): Loss of power supply to these loads does not cause safety or protection issues. They are supplied by Class IV.
- Safety-important components (SIC): Loss of power supply to these components can cause a nuclear safety issue. They are supplied by the relevant Classes I, II, III and are designed considering the safety requirements for SIC electrical loads.
- Investment protection (IP): Loss of power supply to these components will cause an IP issue. They are supplied by the relevant Classes I, II, III.

This comprehensive analysis of electrical loads serves as the foundation for developing reliable models for the power system components. DIgSILENT PowerFactory software was used to model the distribution networks of both DTT and DEMO, incorporating load data. This model accurately represents transformers, transmission lines, and switchboards. By integrating detailed load data, these models simulate the system's response to various scenarios, ensuring the distribution network can effectively handle the unique demands of

the nuclear fusion facility. The insights gained from load characterization process optimize the simulation models (improved accuracy and reliability), leading to a more resilient and adaptable electrical distribution network (better equipped to handle variations in load profiles).

The mathematical foundation of many power engineering applications (such as state estimation, network optimization, voltage control, generation dispatch, etc.) is represented by power flow equations [66], a system of nonlinear equations that describe the steady-state operation of the electrical power system. They are solved by using various iterative methods, such as the Newton-Raphson, Gauss-Seidel and Fast Decoupled methods, each with its own strengths and weaknesses in terms of convergence speed and accuracy.

The PowerFactory software offers specific methods to tackle the power flow problem, including Newton-Raphson with Current Equations and Newton-Raphson with Power Equations (classical). The choice between these methods depends on the type of network being analyzed. In large, heavily loaded transmission systems, the Power Equations formulation typically exhibits better convergence. On the other hand, distribution systems, especially unbalanced ones, tend to benefit more from the Current Equations formulation. However, regardless of the chosen formulation, iterative methods are necessary due to the non-linear nature of the power flow equations.

Traditionally, Power Flow analysis relies on deterministic input data. These variables can either represent a "snapshot" of the system, indicating its state at a specific time, or they can be analyst-defined values based on assumptions, representing expected or desired generation and load profiles for the system under study. This deterministic approach calculates a single solution limited to the chosen input conditions.

However, the configuration of an electrical distribution system is not static but evolves over time to meet the demands of various processes. To obtain more accurate results that account for these changes, an Root Mean Square (RMS) simulation approach was employed for the DTT case study. RMS simulations provide a comprehensive analysis of the effective values of electrical quantities such as voltage and current under varying load conditions. This approach enables the assessment of power quality issues, such as harmonics and phase imbalances, and ensures that the distribution network can effectively handle both steady-state and dynamic load variations.

While deterministic simulations are ideal for optimization under fixed conditions, probabilistic approaches are used to evaluate performance under varying and uncertain scenarios. Together, these methodologies provide a comprehensive toolkit for electrical system design and analysis.

When faced with uncertain input conditions, a multitude of scenarios must be evaluated.

For the DEMO case study, the load uncertainties are mostly related to the design stage of the project. Indeed, unlike DTT, where the installed power is fixed and no longer subject to changes, DEMO loads still need to be largely studied and sized, as they are also derived by extrapolation from similar projects (e.g., ITER).

Conventional power flow analysis methods documented in the literature address the inherent variability and stochastic nature of input data through various approaches, including sampling methods, analytical techniques, and approximate solutions. Among these, uncertainty propagation studies often rely on sampling-based techniques such as Monte Carlo simulation. This method involves running the power flow model numerous times, each with a different combination of randomly sampled input values.

In the sensitivity analysis step, we will identify the input parameters that have the greatest impact on the uncertainty in the output. This information can then be used to improve the design of the electrical infrastructure and reduce the overall uncertainty in the

system performance.

3.1.1 Deterministic Simulations

Deterministic Power Flow (DPF) simulations, encompassing both static and dynamic types, are essential tools in the design and analysis of electrical systems. Static Power Flow simulations focus on the steady-state operation of the power system, analyzing load conditions and ensuring optimal performance under known parameters. In contrast, dynamic simulations assess the system's response to disturbances over time, providing crucial insights into stability and dynamic behavior.

Table 3.1 provides an overview of some of the main transient events that occur in nuclear fusion facilities, categorized by the operational phase in which they typically arise. In such facilities, the electrical system is designed to ensure a stable and reliable power supply for various operations.

With reference to the normal operation scenario, it encompasses the following phases:

- Ramp-up: This period involves gradually increasing the power supply to the plasma until it reaches the desired operational level. During this phase, the Electrical Network System (ENS) experiences significant power transients as the various systems ramp up their energy demands.
- Flat-top: Once the plasma reaches the desired operational level, the power supply is maintained at a relatively constant level for the duration of the flat-top phase. However, even during this seemingly steady state, subtle power fluctuations can occur due to internal adjustments and external disturbances.
- Ramp-down: The ramp-down phase involves gradually decreasing the power supply to the plasma until it reaches a safe level for termination. Similar to the ramp-up phase, this period also presents transient power demands on the ENS.

The flow chart in Figure 3.1 illustrates the process of dynamic RMS power flow simulation, outlining the steps involved, from system parameter definition to the analysis of results.

3.1.2 Probabilistic Simulations

DPF studies examine the state variables of power networks using predetermined input parameters and conditions. In contrast, the PPF study account for uncertainties and randomness within the system. For instance, load demand in distribution systems can vary significantly and these uncertainties can be represented using probability distribution functions (PDFs) [67]. By assigning appropriate PDFs to them, one can predict potential variations in loads and evaluate their impact on the overall network. In PPF studies, power system parameters are treated as random variables. Consequently, the results are determined by varying these parameters.

To accurately represent the real system behaviour, uncertainty modelling approaches, often referred to as sampling techniques, are essentials for quantifying system uncertainties. These uncertainties can arise from several sources, such as random variability over time, missing or incomplete data, and the limitations of mathematical models that do not perfectly represent the system.

PPF methods are generally categorized into three main types:

Table 3.1. Main Transient Events in Nuclear Fusion Facilities.

Category	Transient Event	Description
Normal Operation	Ramp-up	Gradual increase in power supply to the plasma.
	Flat-top	Maintenance of a constant power supply to the plasma.
	Ramp-down	Gradual decrease in power supply to the plasma.
Faulted Operation	Quench	Sudden transition of a superconducting material to a normal conducting state, often caused by an increase in temperature or intense magnetic field, leading to rapid release of stored energy as heat.
	Plasma disruption	Event where the plasma becomes unstable and is rapidly lost from confinement. This can result in a sudden temperature drop and loss of control, potentially causing significant damage to the reactor.
	Loss of coolant accident	Failure of the cooling system for the plasma chamber.
Testing and Conditioning	Plasma formation	Creation of the initial plasma in the chamber.
	Plasma conditioning	Preparation of the plasma chamber for operation.
Maintenance	Planned outages	Scheduled maintenance activities on the fusion facility.
	Unplanned outages	Unscheduled maintenance or emergency repairs.

- Analytical Methods: They linearize power flow equations to work with probability functions, as demonstrated in several studies [68–70]. However, they can be computationally inefficient.
- Approximate Methods: They avoid linearization but reduce the number of evaluation points, minimizing computational and storage burden [70, 71].
- Monte Carlo Simulation (MCS) Methods: They involve repeated deterministic calculations without approximations, potentially requiring more processing time and storage [68, 70, 72, 73]. However, advancements in computing power, have made MCS a widely used method due to its robustness and accuracy [74, 75].

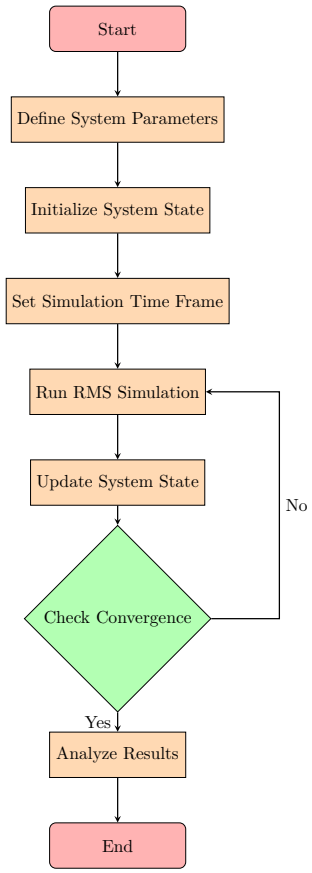

Figure 3.1. Dynamic RMS Power Flow Simulation Flow Chart.

The choice of the most suitable uncertainty modeling approach depends on the specific characteristics of the system being analyzed and the goals of the study. Factors such as system complexity, data availability, and available computational resources should be considered to select the appropriate method. In this work, Monte Carlo-based PPF analysis is considered, due to its advantages. It provides considerable flexibility, allowing it to be applied to various uncertainty modeling problems without the need for specific assumptions regarding the probability distribution of uncertain variables. Additionally, the accuracy of the results improves as the number of simulations increases.

The probabilistic power flow analysis involves the following steps, as illustrated in Figure 3.2.

- Step 1 - Identify and Model Random Variables: Identify all relevant random variables and model their probability distributions. In this case, load power values are assumed to follow a normal distribution with mean μ (base value) and standard deviation σ.
- Step 2 - Set Simulation Parameters: Determine the maximum number of iterations and samples for MCS convergence.
- Step3 - Generate Random Samples: For each iteration, generate random numbers using a suitable algorithm.
- Step 4 - Calculate Fitness Function: Evaluate the fitness function using the generated sample. In PPF analysis, the fitness function is a deterministic power flow analysis.

- Step 5 - Verify Sampling Criteria: Check if the maximum number of samples has been reached. If not, repeat step 3.
- Step 6 - Calculate Expected Values: Calculate the expected value of output variables for each iteration.
- Step 7 - Check Iteration Limit: Verify if the maximum number of iterations has been reached. If not, continue to step 3. Otherwise, terminate the algorithm.

3.1.3 Sensitivity Analysis

The sensitivity analysis, combined with Monte Carlo-based PPF, will identify the input parameters that have the greatest impact on the uncertainty in the output. This information can then be used to improve the design of the electrical infrastructure and reduce the overall uncertainty in the system performance. The methodology adopted will be detailed later in the dedicated paragraph 3.3.

3.2 DTT Case Study

The DTT fusion facility, currently under construction at the ENEA Research Center in Frascati, Italy, is a collaborative effort by the DTT Consortium, involving various scientific and industrial partners, with the scope of exploring solutions to the issue of heat exhaust into the divertor. DTT will be a full-scale tokamak in terms of size and power. A critical aspect of the DTT project is ensuring a robust and efficient ENS capable of meeting its unique power requirements, characterized by high fluctuation and large transients. This section explores the functionalities of the DTT ENS and presents the analyses conducted for its design.

3.2.1 DTT Power Requirements, Grid Connection and Power System Design

DTT operational profile is inherently pulsed, as illustrated in Figure 3.3. The figure shows a typical power demand profile, characterized by a base load of approximately 34 MVA, representing the minimum power required for operation and maintaining magnetic field configurations, and peak power demands reaching nearly 250 MVA during plasma discharge phases. These pulses typically last around 100 seconds, followed by a much longer dwell time (one hour) for plasma current ramp-down and preparation for the next discharge. The total power demand is well within the agreed-upon limit of 300 MVA set by the Italian TSO, which ensures that DTT power requirements can be met without overloading the grid.

The ENS is designed to handle this substantial and fluctuating power demand. Figure 3.4 schematically represents some of the most power-intensive components, including the Heating and Current Drive (HCD) system and the coil Power Supply System (PSS).

As shown in Figure 3.5 and Figure 3.6, the ENS is fed at 150 kV by the National Grid (NG) and is divided into two main sections:

- High Voltage System (HVS): Including the 150-kV underground cable line which connects the primary TSO substation to the HV/MV substation (SS0).

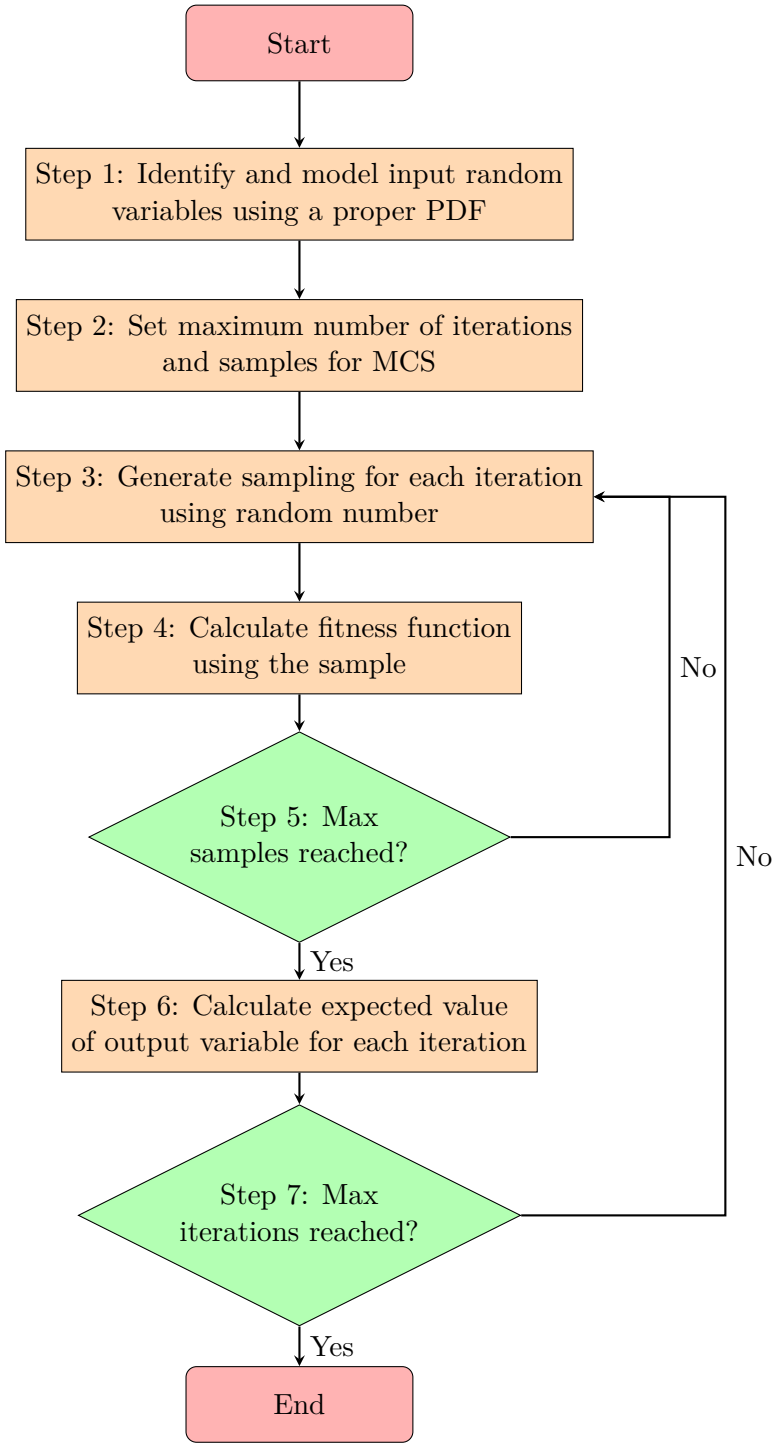

Figure 3.2. Flowchart of the probabilistic analysis algorithm.

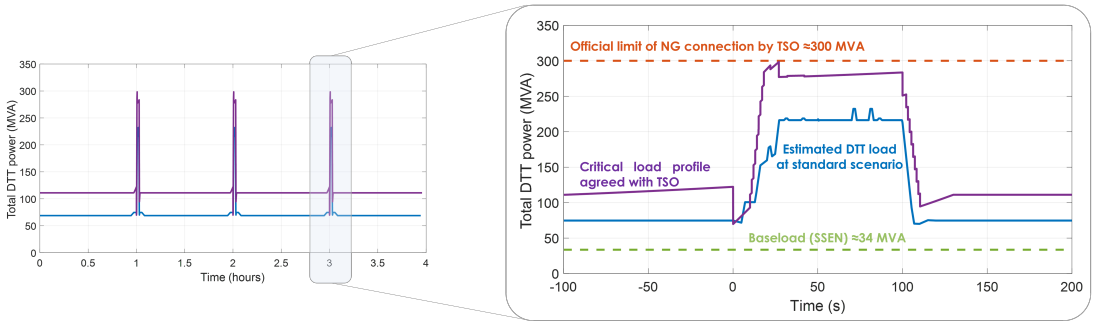

Figure 3.3. DTT duty cycle.

- Electrical Distribution System (EDS): Further subdivided into two sections that are electrically coupled at the HV level, but maintain separate downstream distributions. They are:
  - Steady-State Electrical Network (SSEN): Supplying continuous power to non-pulsed loads.
  - Pulsed Power Electrical Network (PPEN): Designed for pulsed loads like HCD systems, featuring electronic converters for specific waveform control and partial voltage fluctuation compensation.

  This ensures that each load is connected to the dedicated distribution section based on its type.

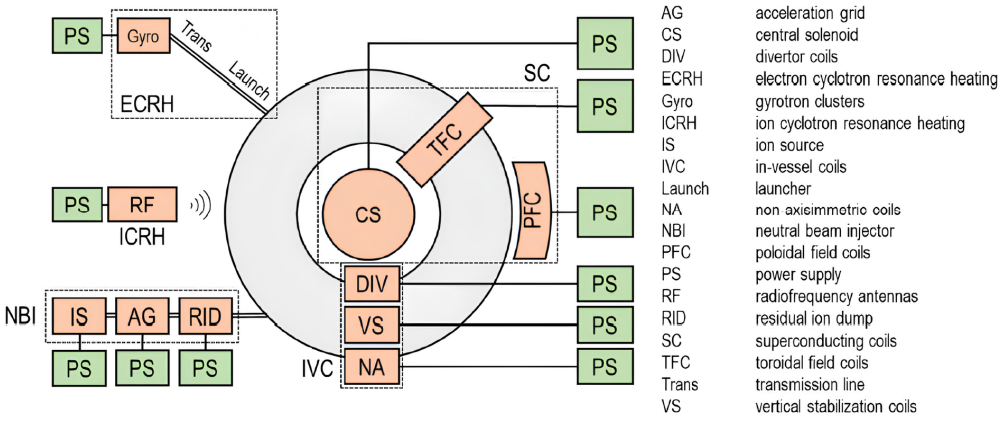

Figure 3.4. Schematics of HCD systems, coils and PSS.

As outlined in Figure 3.5, the SS0 substation houses five 150/21 kV power transformers, each rated at 63 MVA. Four PPEN transformers are designed with an overload capacity of up to 100 MVA for 100 seconds to handle pulsed loads. The remaining transformer supplies steady-state loads and is equipped with on-load tap changers (OLTCs) for voltage adjustment.

Downstream of SS0, the distribution system is arranged using three standard voltage levels: 20 kV, 6 kV, and 400 V (230 V for single-phase loads). Five Load Centers (LCs) are strategically positioned for efficient power distribution, as highlighted in Figure 3.6. However,

not all LCs utilize all voltage levels. For instance, LC3 and LC4 supply LV steady-state loads and receive their power supply from LC5 at 20 kV. Additionally, as depicted by the color scheme in Figure 3.5, pulsed power loads are exclusively supplied by LC1, LC2, and LC5. Specifically, the Neutral Beam Injection (NBI) and Ion Cyclotron Resonance Heating (ICRH) systems are powered by LC2, while the Electron Cyclotron Resonance Heating (ECRH) system receives power from LC5.

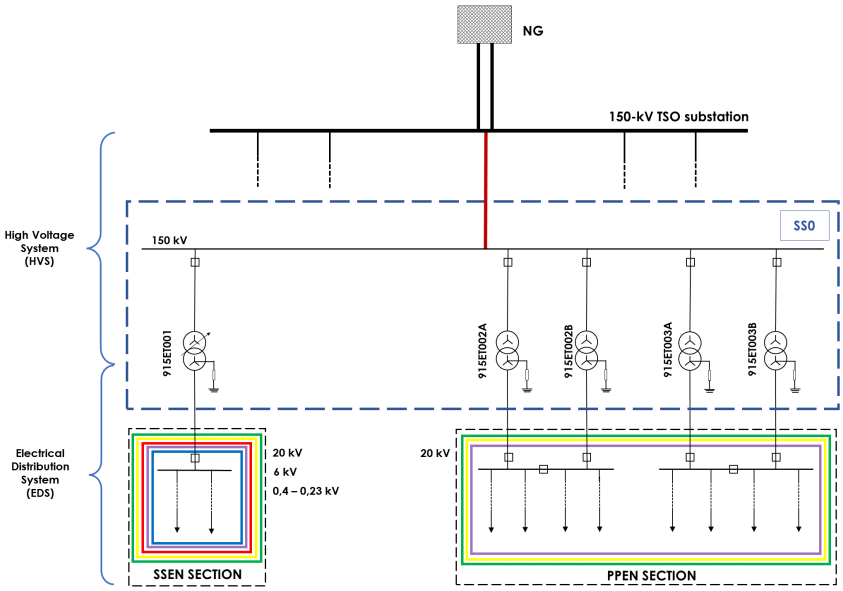

Figure 3.5. Overall Architecture of the DTT Electrical Network System (ENS).

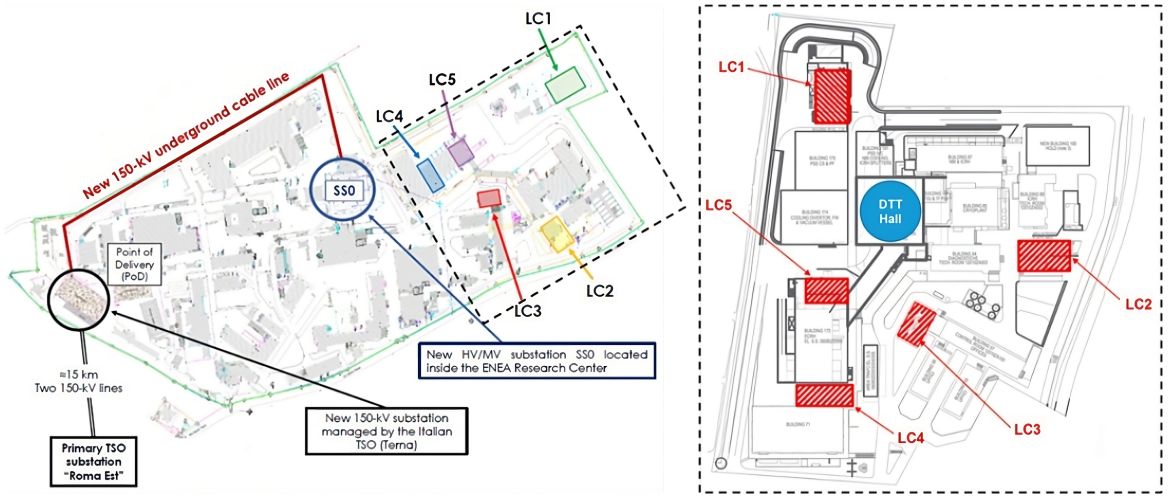

Figure 3.6. Layout of the DTT Electrical Network System (ENS) highlighting Load Centers (LCs).

This configuration results from a continuous optimization based on project advancements, as detailed in references [1–3, 76, 77] and allows the network to manage the large and rapid power transients, ensuring both stability and efficiency.

A simulation model of the ENS, based on the system described in [4], was implemented

using PowerFactory software. This model helped perform static and preliminary dynamic simulations to ensure that the ENS meets operational demands, stability is maintained and the impact on (and from) the NG is minimized.

While previous power flow and fault analyses confirmed the validity of most design choices as documented in references [1–3] (as an example, the rating of transformers is reported in Table 3.2), this section deals with the studies conducted to further optimize the system, including:

- Voltage Impact Study: Investigated the effect of external voltage variations on the DTT EDS by analyzing the system response to different voltage levels at the connection node. This involved running multiple power flow simulations with varying input voltages to identify the operational voltage limits for the electrical equipment, traditionally set at ±10% of the nominal voltage.
- Dynamic Simulation: Assessed the impact of the HCD load duty cycle on the system.

Table 3.2. Transformer Parameters.

Transformation ratio	**Sn [MVA]**	**Pk [kW]**	**Vk [%]**
150±10%/21 kV	63	225	12
20±5%/6.3 kV	15	92	8
	1.25	21	6
20±5%/0.42 kV	2	20	6
	2.5	25	6
0.4±5%/0.42-0.24 kV	0.5	11	4

3.2.2 Voltage Impact Study

Eleven power flow simulations were carried out with different NG voltage conditions, as follows:

- Nominal scenario, with NG voltage V_{NG} equal to 1 p.u., corresponding to the nominal value of 150 kV;
- Ten simulation scenarios with V_{NG} varying from the minimum to the maximum value where the DTT ENS is required max power operate from 0.95 to 1.05 p.u. (±5%).

The simulations were conducted with and without the capacitor banks installed at LV buses to assess their impact on power factor correction and voltage regulation, serving as a preliminary exploration. The design and specifications for a suitable power factor correction system will be determined in future stages.

3.2.3 Dynamic simulation

The power profiles of HCD load clusters were estimated based on a reference operational scenario of power delivered to the plasma by HCD systems (provided by plasma physics studies) depicted in Figure 3.7 and taking into account the characteristics of HCD systems

summarized in Table 3.3, which reports the power contributions and specific operational windows of the various subsystems.

The dynamic simulations were conducted using electromechanical transient RMS simulation in the time domain, as previously illustrated, considering transient stability state variables for machines and converters and SSEN baseload. Also in this case, to assess the system response to varying grid conditions, three scenarios were analyzed, each with a different external grid voltage V_{NG} equal to 1, 0.95, and 1.05 p.u.

An additional simulation was then performed, incorporating a random load profile to simulate the operation of coils responsible for plasma corrections. It was assumed that the correction coils of the PSS have a nominal active power of 50 MW, with ramp-up and ramp-down times of two seconds each, and random variations around the nominal power during the flat top.

Dynamic simulations of voltage and current profiles across the entire network help ensure component operation within limits and identify potential bottlenecks within the ENS that could lead to overloading or voltage instability during transient events.

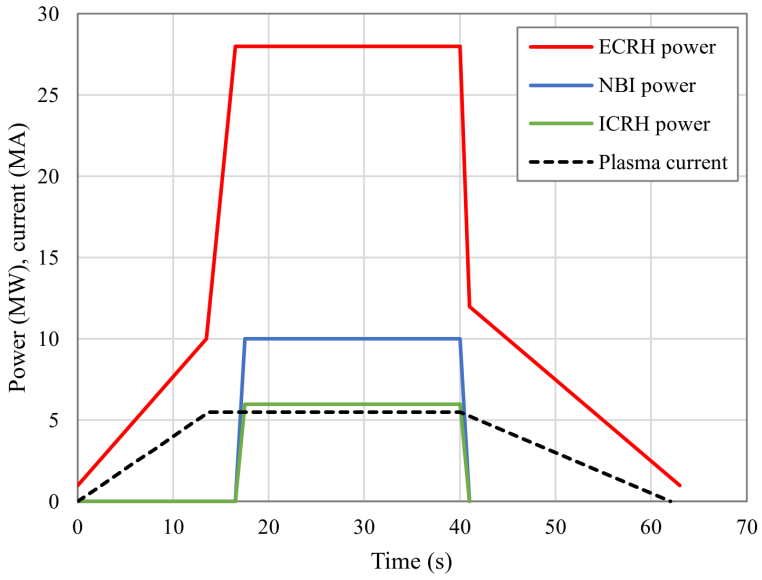

Figure 3.7. Profiles of power delivered to plasma by HCD systems.

Table 3.3. Electrical power characteristics of HCD load clusters.

Subsystem	Start [s]	Stop [s]	S [MVA]	PF	P [MW]
ISPS/RFPS	0	63	9.2	0.97	8.92
PGFPS	0	63	(n.a.)	(n.a.)	0.10
Other	0	63	(n.a.)	(n.a.)	0.02
AGPS	17	63	46.0	0.80	36.80
RIDPS	17	63	1.0	0.97	0.97
EGPS	17	63	(n.a.)	(n.a.)	1.50

3.2.4 Simulation Results

The output of the static voltage analysis (see paragraph 3.2.2) is presented in Tables from 3.4 to 3.8. In detail, voltage values and variations from nominal voltage in LCs are provided, without capacitor banks (Tables 3.4 and 3.5) and with capacitor banks (Tables 3.6 and 3.7). Relative impact of capacitor banks implementation is presented in Table 3.8. The most substantial undervoltage fluctuation on the EDS nodes occurs on LC3 with no utilization of the capacitor banks in the presence of the minimum V_{NG} permissible value. As expected, overvoltages are observed across all the LCs when V_{NG} reaches its maximum value. These overvoltages are notably exacerbated by the activation of capacitor banks, potentially approaching levels that could threaten grid integrity.

Table 3.4. Per unit voltage in static analysis, without capacitor banks (critical cases exceeding ±5% marked).

V_{NG}	**0.95**	**0.96**	**0.97**	**0.98**	**0.99**	**1**	**1.01**	**1.02**	**1.03**	**1.04**	**1.05**
LC1	0.954	0.965	0.975	0.985	0.996	1.006	1.016	1.026	1.037	**1.047**	**1.057**
LC2	0.954	0.964	0.974	0.985	0.995	1.005	1.016	1.026	1.036	**1.047**	**1.057**
LC3	**0.932**	**0.943**	0.953	0.963	0.973	0.983	0.993	1.003	1.013	1.023	**1.034**
LC4	0.961	0.971	0.982	0.992	1.003	1.013	1.023	1.034	1.044	**1.054**	**1.065**
LC5	0.954	0.964	0.974	0.984	0.995	1.005	1.015	1.026	1.036	**1.046**	**1.057**

Results of dynamic simulation (see paragraph 3.2.3) are presented as follows. Figure 3.8a and Figure 3.8b report the active and reactive power absorption profiles considering the NG at its nominal voltage (without and with correction coils PSS contribution).

(see paragraph 3.2.2)

Figure 3.9 reports voltage profiles at PPEN LCs (LC1, LC2, and LC5) at nominal V_{NG}.

Figures from 3.10a to 3.10d present voltage profiles, at nominal V_{NG}, at NG and SSEN feeders (on the MV side of the HV/MV transformer), during operation duty cycle and detailed at start of ramp-up, to analyze effect of load ramp-up towards the grid.

As expected, the voltage exhibits significant fluctuations during the duty cycle due to the presence of variable loads. The analyzed nodes appear to be subject to similar voltage variations. Referring to Figure 3.9, which depicts the voltage variation at pulsed Load Centers, it is evident that the voltage levels remain within acceptable limits, thereby ensuring compliance with relevant standards and guidelines. Figure 3.10 illustrates the voltage magnitude at feeders during the duty cycle, showing how dynamic loading could affect voltage stability on both the external and internal grid. This figure demonstrates the impact of starting and ramping operations on the overall grid performance, which is not compromised as the voltage stays within permissible limits. The variations in voltage magnitude at LCs simulated in the dynamic analysis confirm the values calculated via in the

Table 3.5. Percent deviation from nominal voltage in static analysis, without capacitor banks (critical cases exceeding ±5% marked).

V_{NG}	**0.95**	**0.96**	**0.97**	**0.98**	**0.99**	**1**	**1.01**	**1.02**	**1.03**	**1.04**	**1.05**
LC1	-4.60%	-3.50%	-2.50%	-1.50%	-0.40%	0.60%	1.60%	2.60%	3.70%	4.70%	**5.70%**
LC2	-4.60%	-3.60%	-2.60%	-1.50%	-0.50%	0.50%	1.60%	2.60%	3.60%	4.70%	**5.70%**
LC3	**-6.80%**	**-5.70%**	-4.70%	-3.70%	-2.70%	-1.70%	-0.70%	0.30%	1.30%	2.30%	3.40%
LC4	-3.90%	-2.90%	-1.80%	-0.80%	0.30%	1.30%	2.30%	3.40%	4.40%	**5.40%**	**6.50%**
LC5	-4.60%	-3.60%	-2.60%	-1.60%	-0.50%	0.50%	1.50%	2.60%	3.60%	4.60%	**5.70%**

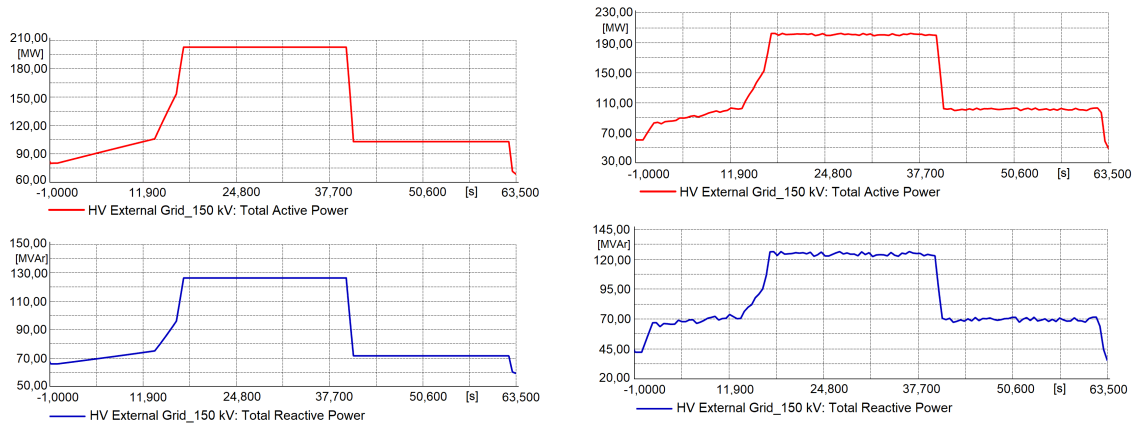

(a) (b)

Figure 3.8. Active and reactive power from NG during duty cycle, without correction coils power supply (a) and with correction coils power supply (b).

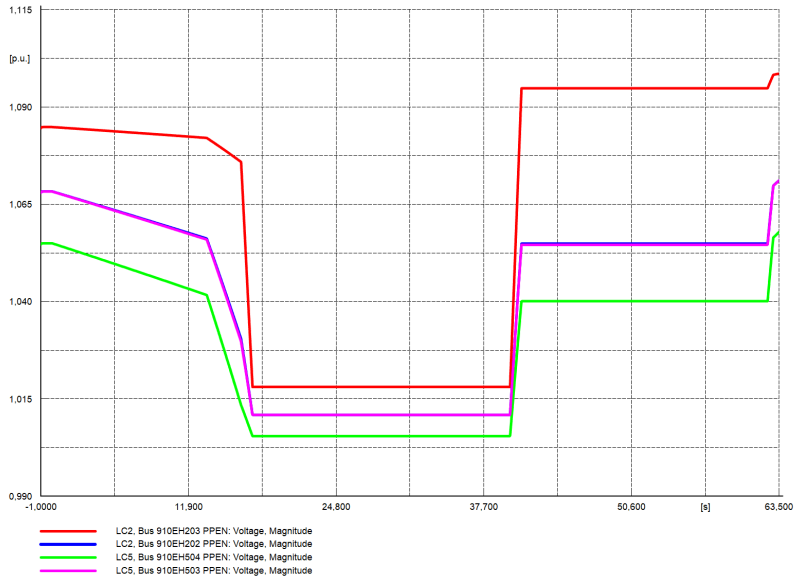

Figure 3.9. Voltage magnitude (p.u.) at PPEN LCs at nominal NG voltage during duty cycle.

Table 3.6. Per unit voltage in static analysis, with capacitor banks (critical cases exceeding ±5% marked).

V_{NG}	**0.95**	**0.96**	**0.97**	**0.98**	**0.99**	**1**	**1.01**	**1.02**	**1.03**	**1.04**	**1.05**
LC1	0.961	0.972	0.982	0.992	1.003	1.013	1.023	1.034	1.044	**1.055**	**1.065**
LC2	0.961	0.971	0.982	0.992	1.002	1.013	1.023	1.033	1.044	**1.054**	**1.065**
LC3	0.958	0.969	0.979	0.989	1	1.01	1.021	1.031	1.041	**1.052**	**1.062**
LC4	0.976	0.987	0.997	1.008	1.018	1.029	1.039	1.05	**1.06**	**1.071**	**1.082**
LC5	0.961	0.971	0.981	0.992	1.002	1.012	1.023	1.033	1.044	**1.054**	**1.064**

Table 3.7. Percent deviation from nominal voltage in static analysis, with capacitor banks (critical cases exceeding ±5% marked).

V_{NG}	**0.95**	**0.96**	**0.97**	**0.98**	**0.99**	**1**	**1.01**	**1.02**	**1.03**	**1.04**	**1.05**
LC1	-3.90%	-2.80%	-1.80%	-0.80%	0.30%	1.30%	2.30%	3.40%	4.40%	**5.50%**	**6.50%**
LC2	-3.90%	-2.90%	-1.80%	-0.80%	0.20%	1.30%	2.30%	3.30%	4.40%	**5.40%**	**6.50%**
LC3	-4.20%	-3.10%	-2.10%	-1.10%	0.00%	1.00%	2.10%	3.10%	4.10%	**5.20%**	**6.20%**
LC4	-2.40%	-1.30%	-0.30%	0.80%	1.80%	2.90%	3.90%	5.00%	**6.00%**	**7.10%**	**8.20%**
LC5	-3.90%	-2.90%	-1.90%	-0.80%	0.20%	1.20%	2.30%	3.30%	4.40%	**5.40%**	**6.40%**

static analysis.

3.3 DEMO Case Study

The DEMO Plant Electrical System (PES), as illustrated in Figure 3.11 (adaptated from [65]), supplies electrical power to all plant loads and delivers surplus power to the Power Transmission Grid (PTG). This involves managing the gross power generation and recirculation to meet internal plant demands. The Turbine Generator (TG), is a unique feature of DEMO, not found in other fusion experiments. It generates power for the PTG and recirculates a portion to supply internal loads. Therefore, DEMO acts as a load or as a generator facility, based on different phases of the plasma scenario [65, 78, 79].

Similar to the categorization described for DTT, the electrical loads within the DEMO system can also be classified into two primary categories: steady-state loads and pulsed loads. Based on the voltage level, the DEMO electrical distribution network is divided into two main parts:

- High Voltage Network (HVN), including all the components contributing to exchange electricity at HV level with the PTG and to deliver it at voltage levels equal to 22 kV and 66 kV;
- Medium and Low Voltage Network (MLVN), including all the components responsible for supplying the necessary electrical power to the plant electrical loads, based on their classifications in terms of nuclear safety (OL, SIC, IP) and additionally including Emergency Diesel Generator (EDG), UPS, and batteries to ensure uninterrupted power in critical situations.

To assess the impact on the PTG at the point of delivery, the focus will be on the electrical distribution sub-network devoted to the supply of steady-state loads (essential for the overall operation of the facility, including offices and other buildings). This sub-network is supplied by 2-windings, 400/23.1 kV step-down power transformers; it distributes 22 kV,

Table 3.8. Percentage difference in voltage between with and without capacitors cases.

V_{NG}	**0.95**	**0.96**	**0.97**	**0.98**	**0.99**	**1**	**1.01**	**1.02**	**1.03**	**1.04**	**1.05**
LC1	0.70%	0.70%	0.70%	0.70%	0.70%	0.70%	0.70%	0.80%	0.70%	**0.80%**	**0.80%**
LC2	0.70%	0.70%	0.80%	0.70%	0.70%	0.80%	0.70%	0.70%	0.80%	**0.70%**	**0.80%**
LC3	2.60%	2.60%	2.60%	2.60%	2.70%	2.70%	2.80%	2.80%	2.80%	**2.90%**	**2.80%**
LC4	1.50%	1.60%	1.50%	1.60%	1.50%	1.60%	1.60%	1.60%	**1.60%**	**1.70%**	**1.70%**
LC5	0.70%	0.70%	0.70%	0.80%	0.70%	0.70%	0.80%	0.70%	0.80%	**0.80%**	**0.70%**

6.6 kV, 0.4 kV (in AC) and 110 V (in DC), each level corresponding to a specific class of loads.

It is to be noted that the feasibility of increasing voltage levels from 22 kV to 33 kV and from 6.6 kV to 11 kV is currently under discussion, as they are regarded as more suitable for DEMO; anyway, the consolidated voltage leves (22 kV and 6.6 kV) are here considered [5, 78, 80].

The grid simulation model has evolved over time to incorporate updates from the data collected in the ELL, considering the following organization:

- 6.6 kV Class IV and Class III loads are supplied by step-down power transformers (22±5x1.25%/6.9 kV up to 40 MVA);
- 0.4 kV Class IV loads are supplied by step-down power transformers (22±5x2.5/0.42 kV up to 2.5 MVA);
- 0.4 kV Class III and Class II loads are supplied by step-down power transformers (6.6±5x2.5/0.42 kV up to 2.5 MVA).

The proper sizing of DEMO distribution network faces challenges due to uncertainties related to power absorption and system parameters [81]. Despite DEMO is in its conceptual design stage, uncertainties are still tied to the estimation of the electrical load power absorption which experimented a high number of changes, following the updates of the project. A graphical representation of this trend is given by the Figure 3.12 and Figure 3.13, showing the variation in DEMO power demand for the steady-state distribution section.

An uncertainty analysis framework using probabilistic simulation techniques is applied to design of the DEMO distribution network. Utilizing Monte Carlo simulations and probability density functions, the framework quantifies uncertainty levels in power absorption from the external grid, offering valuable insights for decision-makers.

3.3.1 Data acquisition and modeling of the elements of the internal grid

The Monte Carlo simulations fulfilled the following conditions:

- Input data to the model: A normal distribution is used to model the variability in active power absorption within each category that vary within a certain range around the rated active power (Eq. 3.1):

$$P \sim \mathcal{N}(\mu, \sigma^2) \tag{3.1}$$

  For the proposed PPF model, μ_i and σ_i are the base load and standard deviation for input variable, respectively, assumed based on the information about rated power and uncertainty coefficients provided in the ELL for various electrical loads.

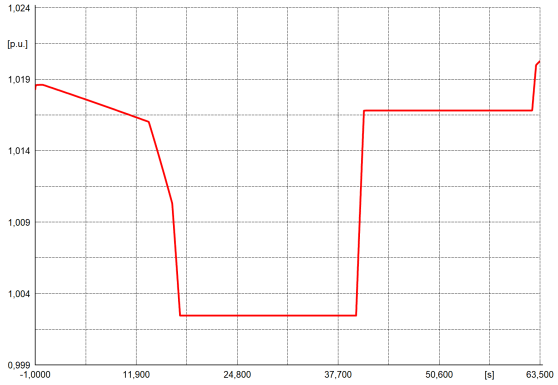

(a) Voltage magnitude in p.u. at NG during duty cycle

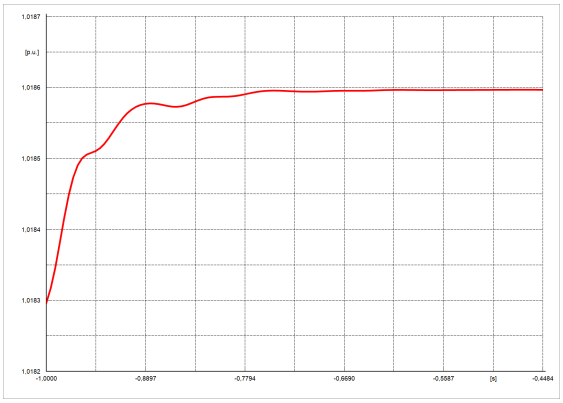

(b) Detail of voltage magnitude in p.u. at NG during start of ramp-up

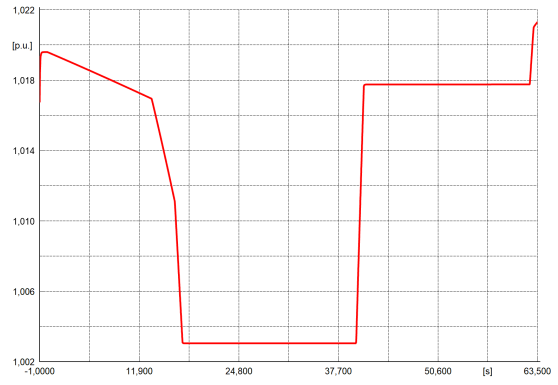

(c) Voltage magnitude in p.u. at SSEN feeder during duty cycle

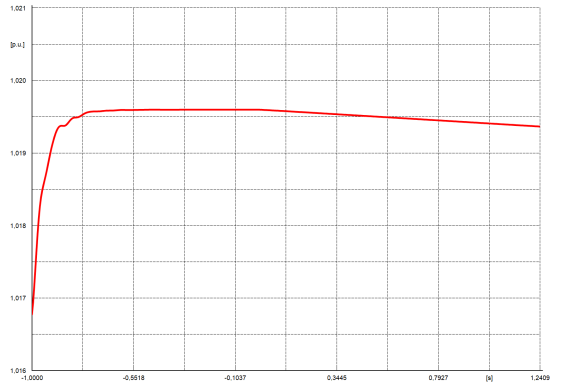

(d) Detail of voltage magnitude in p.u. at SSEN feeder during start of ramp-up

Figure 3.10. Voltage magnitude in p.u. at NG and SSEN feeders during duty cycle and start of ramp-up.

- Load Categorization: Electrical loads are grouped into recurring categories within each subsystem (pumps, cubicles, special loads, etc.).
- Uncertainty coefficients were assigned for each rated power of the electrical loads belonging to the category under consideration. Notably, three qualitative uncertainty levels (High Confidence, Medium Confidence, High Uncertainty) have been defined based on data accuracy and future design revisions. Each level corresponds to a specific uncertainty range (0-20%, 20-60%, and >60% respectively).
- Size of the sample: In the Montecarlo method it remains to the choice of the programmer making the simulation, considering that the more iterations are made, the greater the precision of the probabilities obtained. A number of 1000 samples was chosen as a good trade-off between the quality of the results and the computational time [67, 82].
- Definition of the Case Studies:
  - Case 1: Evaluates the impact of uncertainty coefficients on total power absorption (active and reactive) and transformer sizing.

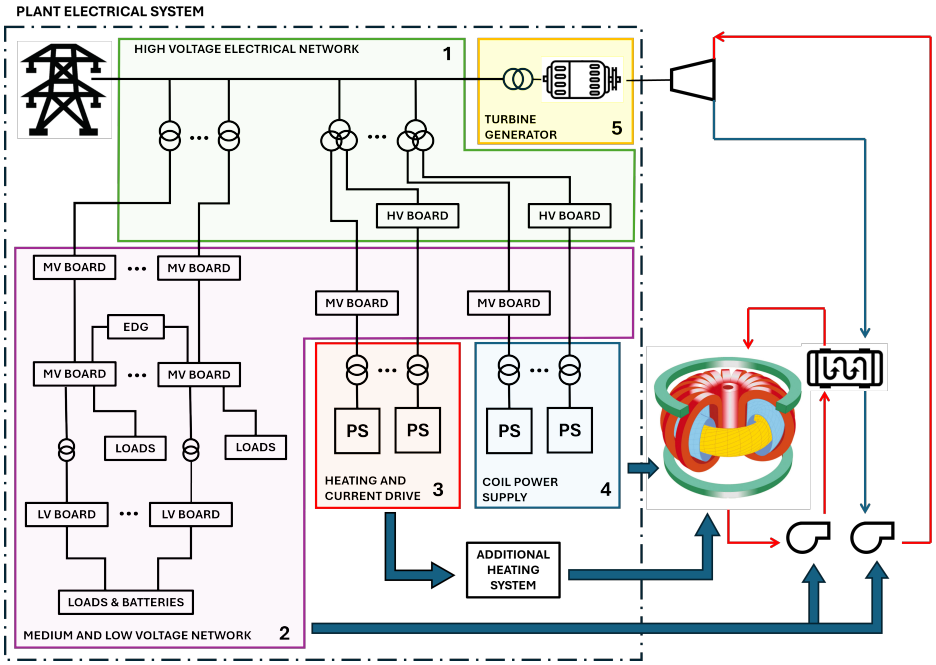

Figure 3.11. Simplified block diagram of the DEMO PES.

– Case 2: Analyzes the contribution of the most significant subsystems (BoP, AUX, BUI) to total power absorption, representing over 80% of its value.

Figure 3.14 and Figure 3.15 illustrate the relative contribution of each subsystem to the overall power consumption. The legend clarifies the color coding scheme used to differentiate the subsystems, which are arranged in a clockwise direction for easy identification.

Once the system is modeled and incorporated to the variability of the load demand in each case, PPF simulations can be made by using the relative tool available in PowerFactory software. The analysis focuses on the internal HVN to MLVN for steady-state loads, investigating the sensitivity of power flow to load assumptions.

3.3.2 Setting of the Simulation Scenarios

Simulations were performed in four different scenarios, based on the coupling options between the Primary Heat Transfer System (PHTS) and the Power Conversion System (PCS). Following latest project updates, two options for the Balance of Plant (BoP) are presently under consideration [81]:

- Helium Cooled Pepple Bed (HCPB) breeding blanket configuration with Indirect Coupling Design option;
- Water Cooled Lithium Lead (WCLL) breeding blanket configuration with Direct Coupling Design option.

In addition, two different phases of the plasma scenario are considered, namely, the Flat-Top and the Dwell Time, regarded as the most and the least demanding one, respectively.

Table 3.9 and Table 3.10 present the rated power values for different electrical systems required to implement the specific coupling options for the two configurations. The data are summarized in the histograms shown in Figure 3.16.

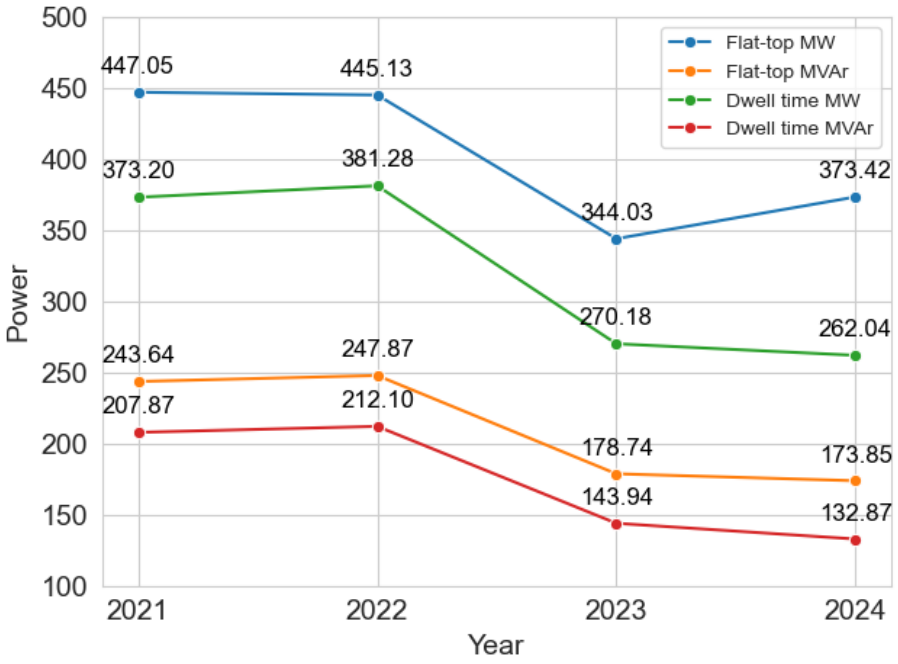

Figure 3.12. Variation in total active and reactive power demand of DEMO for both plasma phases (flat-top and dwell time) in indirect coupling configuration as documented in the ELL from 2021 to 2024.

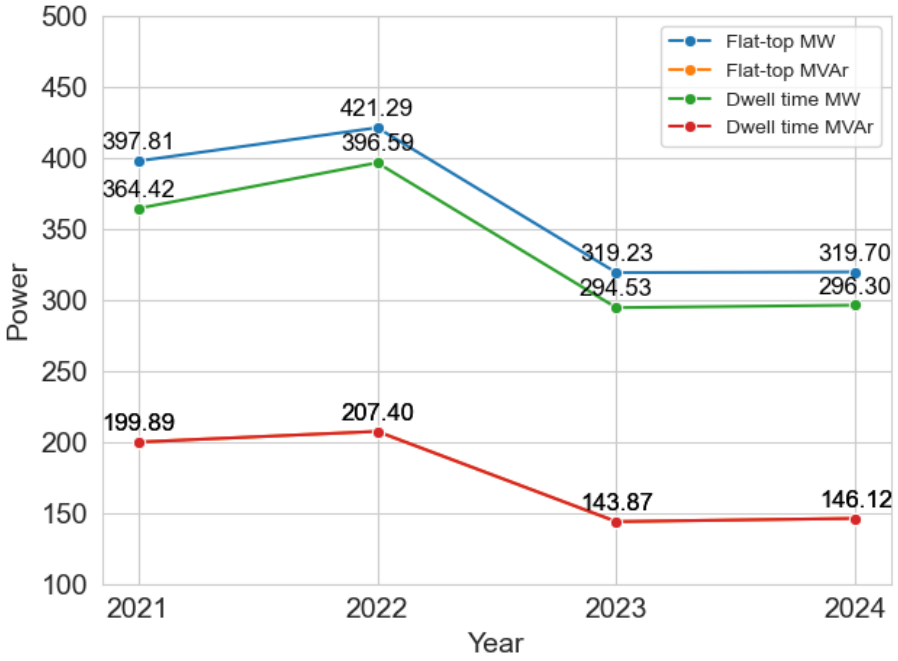

Figure 3.13. Variation in total active and reactive power demand of DEMO for both plasma phases (flat-top and dwell time) in direct coupling configuration as documented in the ELL from 2021 to 2024. The orange curve is not visible because it overlaps with the red curve.

Table 3.9. DEMO subsystems active and reactive power values for indirect coupling scenario (for steady-state loads).

System	Description	Indirect Flat-Top power		Indirect Dwell Time power	
		Active [MW]	Reactive [MVAr]	Active [MW]	Reactive [MVAr]
AUX	Auxiliaries	95.4	46.2	95.4	46.2
BUI	Buildings	56.0	26.9	56.0	26.9
CRYO	Cryoplant and Cryodistribution	20.0	9.7	20.0	9.7
DIA	Diagnostics	0.5	0.3	0.5	0.3
HCD	Heating and Current Drive System	4.0	2.0	4.0	2.0
HCPB ICD BOP	Helium Cooled Pebble Bed Balance of Plant	171.2	64.4	59.1	23.1
PCS	Power Conversion System	4.7	2.25	4.7	2.3
PES	Plant Electrical System	1.8	0.9	1.8	0.9
RM	Remote Maintenance	4.5	2.2	4.5	2.2
TER.HCPB	Tritium Extraction and Removal (HCPB PHTS)	11.4	5.5	11.4	5.5
TFV	Tritium, Fuelling, Vacuum	2.3	1.1	2.3	1.1
	Total	**371.8**	**161.45**	**259.7**	**120.2**

Table 3.10. DEMO subsystems active and reactive power values for direct coupling scenario (for steady-state loads).

System	Description	Indirect Flat-Top power		Indirect Dwell Time power	
		Active [MW]	Reactive [MVAr]	Active [MW]	Reactive [MVAr]
AUX	Auxiliaries	95.4	46.2	95.4	46.2
BUI	Buildings	56.0	26.9	56.0	26.9
CRYO	Cryoplant and Cryodistribution	20.0	9.7	20.0	9.7
DIA	Diagnostics	0.5	0.3	0.5	0.3
HCD	Heating and Current Drive System	4.0	2.0	4.0	2.0
WCLL DCD BOP	Water Cooled Lithium Lead Direct Coupling Design Balance of Plant	120.0	36.4	95.3	36.4
PCS	Power Conversion System	4.7	2.25	4.7	2.3
PES	Plant Electrical System	1.8	0.9	1.8	0.9
RM	Remote Maintenance	4.5	2.2	4.5	2.2
TER.WCLL	Tritium Extraction and Removal (WCLL PHTS)	11.5	5.4	11.5	5.4
TFV	Tritium, Fuelling, Vacuum	2.3	1.1	2.3	1.1
	Total	**320.7**	**133.35**	**296**	**133.4**

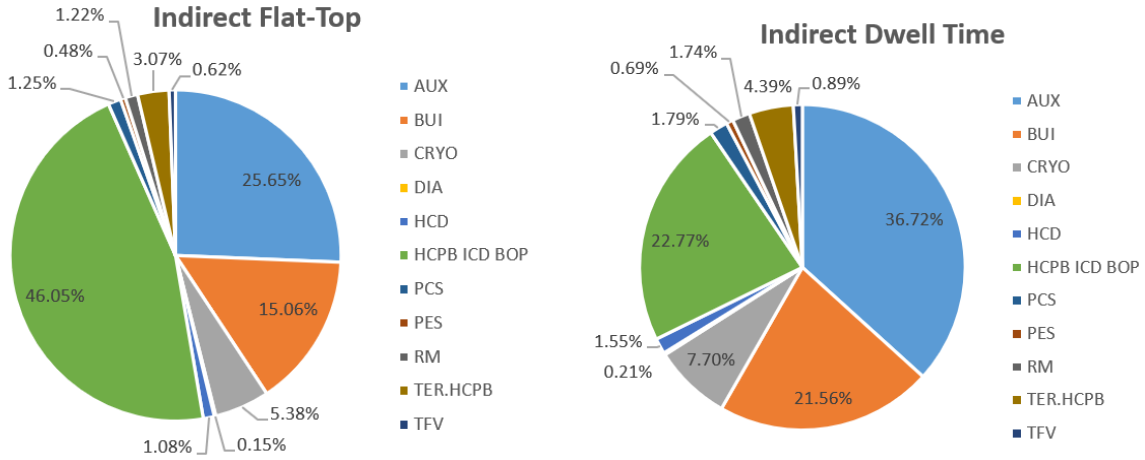

(a) (b)

Figure 3.14. Percentage breakdown of installed power among the various subsystems for the (a) indirect coupling Flat-Top, (b) indirect coupling Dwell-Time scenarios.

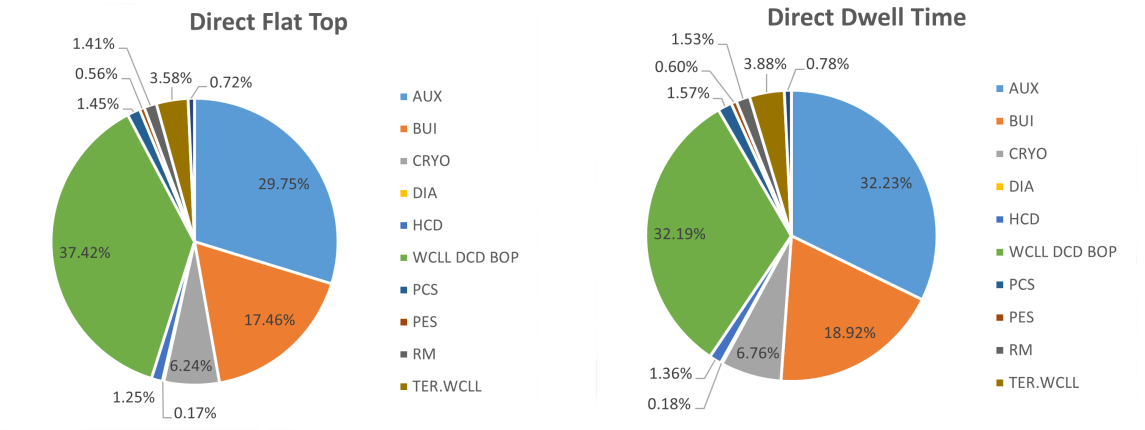

(a) (b)

Figure 3.15. Percentage breakdown of installed power among the various subsystems for the (a) direct coupling Flat-Top, (b) direct coupling Dwell-Time scenarios.

To evaluate how sensitive the HVN/MLVN network is to uncertainties in load demands, a two-step analysis is employed utilizing probabilistic variables for both case studies:

- Step 1: Probabilistic Load Assessment and Overload Check:
  - Monte Carlo simulations are employed to generate probability curves. These curves depict the variability in both active and reactive power absorption from the PTG. Additionally, the simulations provide probability curves for the loading of transformers, including their corresponding mean values, standard deviations, and maximum values.
  - An overload check is conducted using the maximum loading values to identify potential safety concerns. If these values exceed established safe limits for the electrical equipment, it indicates a need to revisit the initial sizing of these components.

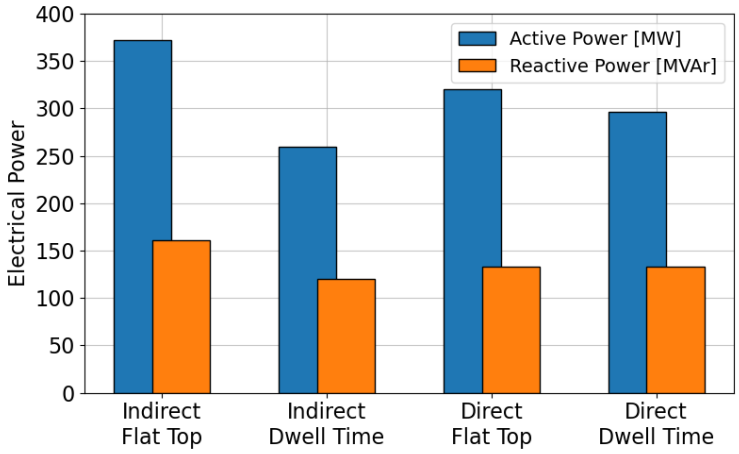

Figure 3.16. Active and reactive power of DEMO steady-state loads for indirect and direct coupling configuration during Flat-Top and Dwell Time plasma phases.

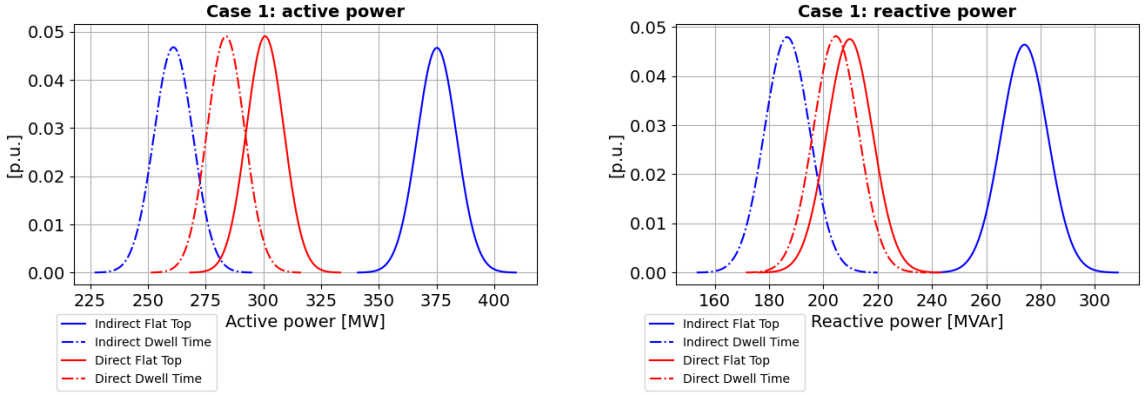

(a) **(b)**

Figure 3.17. Active (a) and Reactive (b) Power Probability Density Functions resulting from Monte Carlo simulations.

- Step 2: Iterative Refinement for Robust Design:

  The simulations are iteratively run after necessary modifications are made to the component sizing based on the overload checks from Step 1. This iterative approach guarantees that adjustments effectively mitigate potential overloading issues identified earlier.

3.3.3 Simulation Outcomes

The model described previously outputs normal distributions for both active and reactive power absorbed from the external grid.

The results of Case 1 are shown in Figure 3.17a and Figure 3.17b. These plots show the probability distributions of active and reactive power absorption for the entire system across different configurations (BoP coupling options) and plasma phases. The trends in the active and reactive power probability curves both follow a normal distribution (with their own mean μ and standard deviation σ) due to the constant power factor relating them.

A key observation is that the spread of the distributions differs between flat-top and dwell-time plasma phases for the HCPB configuration compared to WCLL. The mean values in the two phases are closer for WCLL. This can be primarily attributed to the significant differences in power demand of the loads in the two configurations, rather than the uncertainty itself.

The results in Table 3.11 quantify the mean values and uncertainties (represented by a coverage factor of $\pm 4\sigma$) of the normal distribution curves.

Another finding from Table 3.11 is that the reactive power values exceed the sum of the ELL reactive powers for each plasma phase. This phenomenon can be explained by the contribution of the power transformers to reactive power losses.

Table 3.11. Mean values and associated uncertainties (expressed as percentage deviations) of active and reactive power for the four scenarios investigated in Case 1.

Case 1	**P [MW]**	**ΔP%**	**Q [MVAr]**	**ΔQ%**
Indirect Flat-Top	375 ± 34	±9.1%	274 ± 34	±12.6%
Indirect Dwell-Time	261 ± 34	±13.1%	187 ± 33	±17.8%
Direct Flat-Top	301 ± 33	±10.8%	210 ± 34	±16.0%
Direct Dwell-Time	284 ± 33	±11.5%	205 ± 33	±16.2%

3.3.4 Sensitivity Analysis Results

To evaluate the sensitivity of the HVN/MLVN electrical equipment, a dedicated analysis was conducted using Case 1 input data. This approach, which can be replicated for any network component, is illustrated here with particular reference to power transformers.

The analysis identified the number of transformers exceeding 100% of their rated capacity during the PPF simulations, along with the associated probability of these transformers experiencing overload conditions. Following this identification, a new PPF analysis was performed, by adjusting the commercial size of power transformers where necessary. Notably, these modifications were only applied to transformers exceeding a pre-defined probability threshold (e.g., 30%) for overload.

Table 3.12 reports the types of the power transformers that have a probability exceeding 30% of surpassing their 100% loading capacity during PPF simulations. To address these potential overloads, the size of these transformers was adjusted. These adjustments ensure the transformers operate within acceptable loading ranges during system operation.

The sensitivity analysis also investigated the effects of power uncertainties associated

Table 3.12. Overloaded Critical Transformers exceeding the probability thresholds.

		Loading >100% probability				
Name	**Old Transformer Type**	**Direct Flat-Top**	**Direct Dwell Time**	**Indirect Flat-Top**	**Indirect Dwell Time**	**New Transformer Type**
TR1A BLDG 55	TR 22/6.9 kV 25 MVA	34.37%	34.16%	34.09%	33.02%	TR 22/6.9 kV 31.5 MVA
TR1A BLDG Group1	TR 22/6.9 kV 10 MVA	44.67%	44.16%	44.72%	41.68%	TR 22/6.9 kV 16 MVA
TR1B CRYO BLDG 51	TR 22/0.42 kV 1.25 MVA	37.82%	37.60%	37.88%	36.49%	TR 22/0.42 kV 1.6 MVA
TR1C BLDG 11 pt1	TR 22/0.42 kV 2.5 MVA	71.77%	68.98%	0.00%	0.00%	TR 22/0.42 kV 3.125 MVA
TR1C BLDG 11 pt3	TR 22/6.9 kV 31.5 MVA	42.20%	41.88%	41.98%	40.30%	TR 22/6.9 kV 40 MVA
TR1E BLDG 11 pt1	TR 22/0.42 kV 2.5 MVA	73.87%	71.10%	0.00%	0.00%	TR 22/0.42 kV 3.125 MVA
TR1F BLDG 11 pt3	TR 22/0.42 kV 1.25 MVA	61.71%	60.95%	61.82%	57.23%	TR 22/0.42 kV 1.6 MVA
TR1I BLDG 11 pt1	TR 22/6.9 kV 31.5 MVA	42.99%	42.68%	43.31%	41.06%	TR 22/6.9 kV 40 MVA
TR2A SIC Loads	TR 22/0.42 kV 1.25 MVA	0.02%	0.02%	46.98%	41.37%	TR 22/0.42 kV 1.6 MVA
TR2B SIC Loads	TR 22/0.42 kV 1.6 MVA	46.63%	46.20%	47.42%	44.78%	TR 22/0.42 kV 2 MVA
TR2C SIC Loads	TR 22/0.42 kV 1.6 MVA	46.63%	46.20%	47.42%	44.78%	TR 22/0.42 kV 2 MVA

with the BoP, Auxiliaries (AUX) and Buildings (BUI) subsystems. The results from Case 2 are presented in Figure 3.18a and Figure 3.18b. The analysis explores the relationship between the active and reactive power absorbed by individual electrical subsystems and the overall active power demand on the electrical grid. This analysis is based on regression modeling, assuming a linear relationship between the two variables.

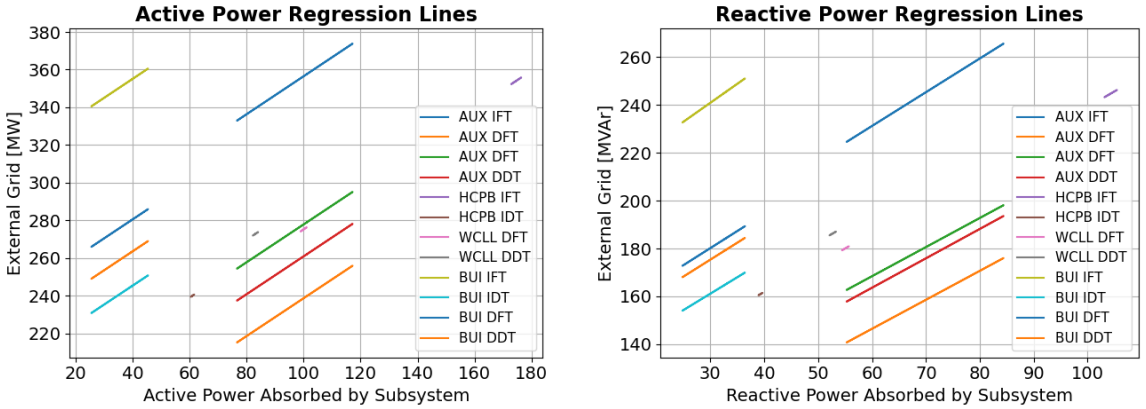

(a) **(b)**

Figure 3.18. Active (a) and reactive (b) power regression lines for electrical subsystems for each simulated scenario for Case 2.

The plot illustrates the relationship between the active (a) and reactive (b) power consumption of each electrical subsystem on the x-axis, while the total active (a) and reactive (b) power demand on the electrical grid, encompassing the power consumption of all subsystems, is depicted on the y-axis. Each colored line represents the regression model for a specific electrical subsystem. The slope of the line indicates the sensitivity of the grid's power demand to changes in the subsystem's power consumption. The higher the slope, the more sensitive the grid is to the power fluctuations of that subsystem, while a lower slope indicates less sensitivity.

The higher level of advancement in the BoP design compared to other subsystems significantly reduces the uncertainty associated with its electrical loads. This translates to a narrow range of power consumption for the BoP loads, even though these systems have significant power demands. Conversely, the AUX subsystem has a substantial impact on the power exchanged with the external grid due to its very high requested power and associated high uncertainties. This combination significantly influences total uncertainty, despite the higher installed power of the BoP. Similar considerations can be drawn for the BUI subsystem, although its impact is lower due to its lower installed power.

Chapter 4

Conclusions and Future Developments

This thesis explored the intricate landscape of fusion energy, focusing on its technological, economic and environmental dimensions, alongside a novel study that optimizes the design of power distribution systems within fusion power plants.

The economic viability of fusion power was analyzed in *Chapter 1*, where we explored cost projections, economic models, and the potential socioeconomic impacts of large-scale fusion deployment. By examining case studies and techno-economic assessments, we underscored the importance of continued investment in research and development to drive down costs and facilitate the commercialization of fusion energy. The potential benefits of fusion in mitigating climate change and reducing greenhouse gas emissions was also discussed, highlighting its role in achieving global energy sustainability goals outlined in the Paris Agreement. The journey continued with an examination of the fundamental principles underlying magnetic confinement fusion and the technological advancements that have brought us closer to harnessing the power of the stars. Through comprehensive reviews of reactor designs, including tokamaks and stellarators, and insightful analyses of plasma physics, we have underscored the promising potential of fusion as a sustainable energy source for the future.

Chapter 2 shifted focus to regulatory and safety aspects inherent in fusion power plants. Drawing parallels with established nuclear safety frameworks, we emphasized the importance of stringent safety protocols and regulatory oversight to ensure the safe operation and public acceptance of fusion reactors.

The core of the thesis is discussed in *Chapter 3* focusing on power system studies for fusion facilities, with an emphasis on optimizing the electrical distribution systems within these complex environments. The chapter outlines a comprehensive methodology for assessing and improving the electrical infrastructure, which is crucial for the safe and efficient operation of NFPPs. Starting from a system characterization, based on a detailed analysis of the electrical distribution network including load profiles and grid interconnections, accurate models of various system components have been created. Both deterministic and probabilistic simulations have been employed to analyze the behavior of the power system under different conditions. Deterministic Power Flow (DPF) simulations are used to assess the system's performance under predefined conditions, while Probabilistic Power Flow (PPF) simulations account for uncertainties and variability in load demand, providing a more comprehensive analysis.

A key innovation is the introduction of an uncertainty analysis framework that evaluates both deterministic and probabilistic aspects. By integrating Monte Carlo simulations and

probability density functions, it quantifies uncertainties in key parameters, aiding decision-making regarding system resilience and performance. Furthermore, this framework ensures that voltage profiles consistently meet desired thresholds, even with fluctuating conditions, enhancing grid resilience.

The proposed methodology offers a significant advantage for designing robust HVN/MLVN networks by enabling quantitative risk assessment through probability curves. This approach reveals the likelihood of exceeding safe loading limits under uncertain conditions, providing a more accurate, data-driven alternative to the conservative estimates traditionally used.

The practical application of the proposed methodologies is demonstrated through the case studies of DTT and DEMO projects. In the DTT case study, the analysis focused on power requirements, grid connection, and power system design, with simulations providing valuable insights into voltage impacts and dynamic stability across various operational scenarios. The DEMO case study involved a comprehensive probabilistic analysis to assess uncertainties in power demand and absorption, highlighting critical factors influencing grid stability and reliability. A sensitivity analysis revealed the significant impact of specific subsystems on overall grid performance, guiding the optimization of component sizing and network configuration.

The developed methodologies offer substantial improvements over traditional approaches to power distribution in NFPPs, providing a more nuanced understanding of operational risks and performance expectations in fusion energy systems. This data-driven approach enables more informed decision-making, which is crucial for the safe and efficient design of future fusion power plants. The research also aligns with the strategic goals of the EUROfusion roadmap by addressing key challenges in the integration of fusion energy into existing power grids. The insights gained from the DTT and DEMO studies are directly applicable to ongoing and future projects, paving the way for more reliable and economically viable fusion energy solutions. Future research should build on these findings, exploring further refinements in simulation models and extending the analysis to other fusion projects under development. The ultimate goal remains the successful integration of fusion energy into the global energy mix, contributing to a sustainable and carbon-neutral future.

Appendix

A.1 Other Research Activities in EUROfusion project

During my PhD studies, I participated in research activities within the framework of the EUROfusion-supported European project for DEMO. My specific contributions included:

- Updating the data related to DEMO loads reported in the ELL and the associated simulation model of the distribution system developed in PowerFactory.
- Studying available ITER documents to evaluate an ITER-like approach to the design of DEMO's electrical distribution system.
- Developing a Monte Carlo probabilistic model to assess the variation in power demand from DEMO on the European grid. This work started during my training period abroad at the Max Planck Institute for Plasma Physics (IPP) in Garching and focused on analyzing how different assumptions regarding electrical loads could impact decisions concerning the internal distribution system's layout.

A.2 Visiting Period Abroad

Supported by a Sapienza University grant awarded under the "Call for funding research projects for mobility abroad", I spent three months (May to July 2023) at the Max Planck Institute for Plasma Physics (IPP) in Garching, Munich. My research focused on the project titled "Modelling, simulation, and analysis of the electrical distribution system of the DEMO nuclear fusion reactor and its connection to the grid". This work was conducted within the DEMO Work Package Plant Electrical Systems (WPPES) and DEMO Central Team (DCT). My primary objective was to contribute to preliminary studies for the design of the SSEN of DEMO, aiming to create a simulation model to optimize the layout of the internal distribution network. After identifying the main electrical loads, understanding their characteristics was crucial for choosing the best network configuration. A Probabilistic Power Flow analysis was performed to assess the overall impact of intrinsic uncertainty in the energy consumption profiles of various subsystems. The goal was to establish a range of fluctuations in the overall absorption profile and verify how such uncertainties could influence design choices for the internal distribution network. The mission's objectives were translated into the following activities:

- Definition and characterization of loads powered by the SSEN to update the DEMO ELL. In some cases, when information was not yet available, data were extrapolated from the ITER project. This activity required close collaboration with Project Leaders (PLs) and System Design Leaders (SDLs). It was also essential to conduct an in-depth

study of the operation of various DEMO systems and their interactions, considering regulations for nuclear electrical installations to ensure full compliance with safety requirements. Finally, support was provided to the Project Management Unit (PMU) and the PL of the Electrical System in contractual activities with industry related to the layout of the DEMO Tokamak Building, through participation in meetings, drafting reports, and discussing and validating the ELL with the PLs of various systems.

- Study and analysis for sizing diesel generators and studying the sequence of restoring safety electrical loads after the loss of external power.
- Development of probabilistic models and analysis of power flow and short circuits on the SSEN by implementing simulation models in the DIgSILENT PowerFactory software environment to verify and optimize the most suitable design solutions.
- Contribution to the development of the preliminary electrical diagram of the power supply system for Volumetric Neutron Source (VNS), an experimental nuclear plant designed to validate critical technological solutions for future nuclear fusion reactors.
- Contribution to the preliminary sizing of the Fast Discharge Unit (FDU) for VNS. The FDU is essential for quickly extracting energy during quenching, a phenomenon where a superconductor loses its superconducting state, causing temperature spikes that spread through the magnet and damage it.

A.3 Scientific Publications

- M. Caldora, G. Greco, M. C. Falvo, G. Marelli, S. Bigioni, S. Caucci, A. Trotta, R. Romano, P. Zito, A. Lampasi, "Power systems for the DTT nuclear fusion experiment," 2021 EEEIC International Conference on Environment and Electrical Engineering.
- M. Caldora, M. C. Falvo, A. Lampasi, G. Marelli, "Preliminary design of the electrical power systems for DTT nuclear fusion plant," Applied Sciences (Switzerland), 2021, 11(12), 5446.
- M. Caldora, L. Cantoni, M. C. Falvo, A. Coretti, A. Lazzarin, C. Vergine, A. Cinque, B. Aluisio, "Synchronous condensers with flywheel for power systems with high penetration of RES: the case of Italian transmission grid," 2022 AEIT International Annual Conference (AEIT). IEEE, 2022.
- M. Caldora, G. Greco, R. Romano, S. Minucci, A. Lampasi, M. C. Falvo, "Progress in the Design of the DTT Electrical Distribution System," 2022 IEEE 21st Mediterranean Electrotechnical Conference (MELECON).
- M. Caldora, M. Manganelli, M. C. Falvo, S. Minucci, A. Lampasi, R. Romano, "Preliminary Sizing and Operation Analysis of the DTT Electrical Network System," in 2023 IEEE International Conference on Environment and Electrical Engineering and 2023 IEEE Industrial and Commercial Power Systems Europe (EEEIC/I&CPS Europe) (pp. 1-6). IEEE (2023, June).
- E. Benedetti, A. Lampasi, S. Pipolo, M. C. Falvo, M. Caldora and A. Trotta, "Analysis for the Integration of the Toroidal Field Power Supply in the DTT Nuclear Fusion Facility," 2023 AEIT International Annual Conference (AEIT), Rome, Italy, 2023, pp. 1-6.

- Ferro, Alberto, et al. "Overview on the Applicability of the ITER/NPP-Like Technologies to the DEMO Plant Electrical System and Promising Alternatives." IEEE Transactions on Plasma Science (2024).
- M. Caldora, S. Panella, M. C. Falvo, S. Minucci, A. Ferro, T. Franke, "A sensitivity analysis on design of the EU-DEMO steady-state electrical power distribution grid via Monte Carlo-based probabilistic power flow models", submitted to the scientific journal *IEEE Access*.

Bibliography

[1] Marzia Caldora, Gabriele Greco, Maria Carmen Falvo, Gianluca Marelli, Stefano Bigioni, Stafano Caucci, Antonio Trotta, Roberto Romano, Pietro Zito, and Alessandro Lampasi. Power systems for the dtt nuclear fusion experiment. In *2021 IEEE International Conference on Environment and Electrical Engineering and 2021 IEEE Industrial and Commercial Power Systems Europe (EEEIC/I&CPS Europe)*, pages 1–5. IEEE, 2021.

[2] Marzia Caldora, Maria Carmen Falvo, Alessandro Lampasi, and Gianluca Marelli. Preliminary design of the electrical power systems for dtt nuclear fusion plant. *Applied Sciences*, 11(12):5446, 2021.

[3] Marzia Caldora, Simone Minucci, Gabriele Greco, Alessandro Lampasi, Roberto Romano, and Maria Carmen Falvo. Progress in the design of the dtt electrical distribution system. In *2022 IEEE 21st Mediterranean Electrotechnical Conference (MELECON)*, pages 501–505, 2022.

[4] Marzia Caldora, Matteo Manganelli, Maria Carmen Falvo, Simone Minucci, Alessandro Lampasi, and Roberto Romano. Preliminary sizing and operation analysis of the dtt electrical network system. In *2023 IEEE International Conference on Environment and Electrical Engineering and 2023 IEEE Industrial and Commercial Power Systems Europe (EEEIC / I&CPS Europe)*, pages 1–6, 2023.

[5] Alberto Ferro, Thomas Franke, Elena Gaio, Stefano Bifaretti, Fabio Bignucolo, Roberto Biondi, Pablo Bravo Rodriguez, Marzia Caldora, Zhe Chen, Mattia Dan, Marco De Nardi, Maria Carmen Falvo, Damien Fasel, Ramon Iturbe Uriarte, Alessandro Lampasi, Francesco Lunardon, Kaiqi Ma, Antonio Magnanimo, Alberto Maistrello, Matteo Manganelli, Simone Minucci, Fabio Ottonello, Stefano Panella, Sabino Pipolo, Mauro Recchia, Felipe Gonzalez Rouco, Francesco Santoro, Segismundo Seijas Portela, Cristina Terlizzi, Roberto Turri, Yanbo Wang, Hanwen Zhang, Pietro Zito, Gianfranco Federici, Sergio Ciattaglia, Luciana Barucca, and Valentina Corato. Overview on the applicability of the iter/npp-like technologies to the demo plant electrical system and promising alternatives. *IEEE Transactions on Plasma Science*, pages 1–8, 2024.

[6] Pieter Tielens and Dirk Van Hertem. Grid inertia and frequency control in power systems with high penetration of renewables. In *Young Researchers Symposium in Electrical Power Engineering, Date: 2012/04/16-2012/04/17, Location: Delft, The Netherlands*, 2012.

[7] Francesco Romanelli, P Barabaschi, D Borba, G Federici, L Horton, R Neu, D Stork, H Zohm, et al. Fusion electricity: A roadmap to the realization of fusion energy. 2012.

[8] McKinsey & Company. Global energy perspective 2023, 2023. `https://www.mckinsey.com/industries/oil-and-gas/our-insights/global-energy-perspective-2023` (Accessed on: June 2024).

[9] Paris Agreement. Paris agreement. In *Report of the Conference of the Parties to the United Nations Framework Convention on Climate Change (21st session, 2015: Paris). Retrieved December*, volume 4, page 2017. HeinOnline, 2015.

[10] M Allen, OP Dube, W Solecki, F Aragón-Durand, W Cramer, S Humphreys, M Kainuma, et al. Special report: Global warming of 1.5 c. *Intergovernmental Panel on Climate Change (IPCC)*, 2018.

[11] I Cook, D Maisonnier, NP Taylor, DJ Ward, P Sardain, L Di Pace, L Giancarli, S Hermsmeyer, P Norajitra, R Forrest, et al. European fusion power plant studies. *Fusion science and technology*, 47(3):384–392, 2005.

[12] Thomas Griffiths, Richard Pearson, Michael Bluck, and Shutaro Takeda. The commercialisation of fusion for the energy market: a review of socio-economic studies. *Progress in Energy*, 2022.

[13] Farrokh Najmabadi, A Abdou, L Bromberg, T Brown, VC Chan, MC Chu, F Dahlgren, L El-Guebaly, P Heitzenroeder, D Henderson, et al. The aries-at advanced tokamak, advanced technology fusion power plant. *Fusion Engineering and Design*, 80(1-4):3–23, 2006.

[14] Winston E Han and David J Ward. Revised assessments of the economics of fusion power. *Fusion Engineering and Design*, 84(2-6):895–898, 2009.

[15] C Bustreo, G Casini, G Zollino, T Bolzonella, and R Piovan. Fresco, a simplified code for cost analysis of fusion power plants. *Fusion Engineering and Design*, 88(12):3141–3151, 2013.

[16] O Crofts and J Harman. Maintenance duration estimate for a demo fusion power plant, based on the efda wp12 pre-conceptual studies. *Fusion Engineering and Design*, 89(9-10):2383–2387, 2014.

[17] Keii Gi, Fuminori Sano, Keigo Akimoto, Ryoji Hiwatari, and Kenji Tobita. Potential contribution of fusion power generation to low-carbon development under the paris agreement and associated uncertainties. *Energy Strategy Reviews*, 27:100432, 2020.

[18] Kathleen Vaillancourt, Maryse Labriet, Richard Loulou, and Jean-Philippe Waaub. The role of nuclear energy in long-term climate scenarios: An analysis with the world-times model. *Energy Policy*, 36(7):2296–2307, 2008.

[19] P Muehlich and T Hamacher. Global transportation scenarios in the multi-regional efda-times energy model. *Fusion engineering and design*, 84(7-11):1361–1366, 2009.

[20] Edgard Gnansounou and Denis Bednyagin. Multi-regional long-term electricity supply scenarios with fusion. *Fusion science and technology*, 52(3):388–393, 2007.

[21] D Turnbull, Alexander Glaser, and Robert James Goldston. Investigating the value of fusion energy using the global change assessment model. *Energy Economics*, 51:346–353, 2015.

[22] K Tokimatsu, Y Asaoka, S Konishi, J Fujino, Y Ogawa, K Okano, S Nishio, T Yoshida, R Hiwatari, and K Yamaji. Studies of breakeven prices and electricity supply potentials of nuclear fusion by a long-term world energy and environment model. *Nuclear Fusion*, 42(11):1289, 2002.

[23] Koji Tokimatsu, Jun'ichi Fujino, Satoshi Konishi, Yuichi Ogawa, and Kenji Yamaji. Role of nuclear fusion in future energy systems and the environment under future uncertainties. *Energy Policy*, 31(8):775–797, 2003.

[24] Helena Cabal, Y Lechón, C Bustreo, F Gracceva, M Biberacher, D Ward, D Dongiovanni, and Poul Erik Grohnheit. Fusion power in a future low carbon global electricity system. *Energy Strategy Reviews*, 15:1–8, 2017.

[25] Gcam - global change analysis model. `https://gcims.pnnl.gov/modeling/gcam-global-change-analysis-model`. Accessed on: March 2024.

[26] Joint Global Change Research Institute. Overview of the global change assessment model (gcam). `<https://unece.org/fileadmin/DAM/energy/se/pdfs/CSE/PATHWAYS/2019/ws_Consult_14_15.May.2019/supp_doc/PNNL-GCAM_model.PDF>`. Presented at the Pathways to Sustainable Energy Stakeholder Consultation Workshop, Bishkek, Kyrgyzstan, 12-14 June 2018. Accessed on: March 2024.

[27] David Pearson Turnbull. *Identifying new saturation mechanisms hindering the development of plasma-based laser amplifiers utilizing Stimulated Raman Backscattering*. PhD thesis, Princeton University, 2013.

[28] Dne21 - integrated assessment model. `https://www.iamconsortium.org/resources/model-resources/dne21/`. Accessed on: March 2024.

[29] MAGICC. `https://magicc.org/`. Accessed on: 23/03/2024.

[30] K Akimoto. Analyses on japan's ghg emission reduction target for 2050 in light of the 2 ∘ c target stipulated in the paris agreement. *J Jpn Soc Energy Resour*, 38(1):1, 2017.

[31] Fusenet Wiki. Beta, 2024. Accessed: 2024-06-23.

[32] Santacruz Banacloche, Ana R Gamarra, Yolanda Lechon, and Chiara Bustreo. Socioeconomic and environmental impacts of bringing the sun to earth: A sustainability analysis of a fusion power plant deployment. *Energy*, 209:118460, 2020.

[33] Wassily Leontief, Erik Dietzenbacher, and Michael L Lahr. *Wassily Leontief and input-output economics*. Cambridge University Press, 2004.

[34] Marcel P Timmer, Erik Dietzenbacher, Bart Los, Robert Stehrer, and Gaaitzen J De Vries. An illustrated user guide to the world input–output database: the case of global automotive production. *Review of International Economics*, 23(3):575–605, 2015.

[35] Gandolfo Alessandro Spagnuolo, Lorenzo Virgilio Boccaccini, Gaetano Bongiovì, Fabio Cismondi, and Ivan Alessio Maione. Development of load specifications for the design of the breeding blanket system. *Fusion Engineering and Design*, 157:111657, 2020.

[36] W.R. Meier, A.M. Dunne, K.J. Kramer, S. Reyes, and T.M. Anklam. Fusion technology aspects of laser inertial fusion energy (life). *Fusion Engineering and Design*, 89(9):2489–2492, 2014. Proceedings of the 11th International Symposium on Fusion Nuclear Technology-11 (ISFNT-11) Barcelona, Spain, 15-20 September, 2013.

[37] George H Miller, Edward I Moses, and Craig R Wuest. The national ignition facility. *Optical Engineering*, 43(12):2841–2853, 2004.

[38] Sergey A. Egorov, Igor Y. Rodin, Nikolay A. Shatil, and Elena R. Zapretilina. Chapter 5 - superconducting magnet systems. In Vasilij Glukhikh, Oleg Filatov, and Boris Kolbasov, editors, *Fundamentals of Magnetic Thermonuclear Reactor Design*, Woodhead Publishing Series in Energy, pages 117–177. Woodhead Publishing, 2018.

[39] RJ La Haye, R Fitzpatrick, TC Hender, AW Morris, JT Scoville, and TN Todd. Critical error fields for locked mode instability in tokamaks. *Physics of Fluids B: Plasma Physics*, 4(7):2098–2103, 1992.

[40] M.S. Tekula and L. Bromberg. Mhd-driven internal coils for tokamak divertor operation. In *15th IEEE/NPSS Symposium. Fusion Engineering*, volume 2, pages 1134–1137 vol.2, 1993.

[41] Emilio Acampora, Raffaele Albanese, Roberto Ambrosino, Antonio Castaldo, Paolo Innocente, and Vincenzo Paolo Loschiavo. Conceptual design of in-vessel divertor coils in dtt. *Fusion Engineering and Design*, 193:113651, 2023.

[42] Yueqiang Liu, CJ Ham, A Kirk, Li Li, A Loarte, DA Ryan, Youwen Sun, W Suttrop, Xu Yang, and Lina Zhou. Elm control with rmp: plasma response models and the role of edge peeling response. *Plasma Physics and Controlled Fusion*, 58(11):114005, 2016.

[43] Iter newsline - design of iter's in-vessel coils converging. `https://www.iter.org/newsline/151/469` (Accessed on: June 2024).

[44] Archie A Harms. *Principles of fusion energy*. Allied Publishers, 2002.

[45] Jt-60sa home page. `https://www.jt60sa.org/wp/` (Accessed on: June 2024).

[46] Broader approach agreement. `https://www.ba-fusion.org/ba/` (Accessed on: June 2024).

[47] John Wesson. The science of jet. *Abingdon, Oxon, OX14 3EA, UK*, 2000.

[48] Ftu home page. `https://web.archive.org/web/20060508112157/http://ftu.frascati.enea.it/index.html` (Accessed on: June 2024).

[49] G. Pucella et al. Overview of the ftu results. *Nuclear Fusion*, 59(11):112015, jul 2019.

[50] Dtt home page. `https://www.dtt-project.it/` (Accessed on: June 2024).

[51] Iter home page. `https://www.iter.org/` (Accessed on: June 2024).

[52] Valerij A. Belyakov, Anatolij B. Mineev, and Victor A. Bykov. Chapter 2 - facilities with magnetic plasma confinement. In Vasilij Glukhikh, Oleg Filatov, and Boris Kolbasov, editors, *Fundamentals of Magnetic Thermonuclear Reactor Design*, Woodhead Publishing Series in Energy, pages 7–37. Woodhead Publishing, 2018.

[53] Anatolij B. Mineev. Chapter 9 - plasma heating systems. In Vasilij Glukhikh, Oleg Filatov, and Boris Kolbasov, editors, *Fundamentals of Magnetic Thermonuclear Reactor Design*, Woodhead Publishing Series in Energy, pages 281–290. Woodhead Publishing, 2018.

[54] Georgij L. Saksagansky and Boris N. Kolbasov. Chapter 6 - vacuum and tritium system. In Vasilij Glukhikh, Oleg Filatov, and Boris Kolbasov, editors, *Fundamentals of Magnetic Thermonuclear Reactor Design*, Woodhead Publishing Series in Energy, pages 179–209. Woodhead Publishing, 2018.

[55] Entso-e - network codes webpage. `https://www.entsoe.eu/network_codes/` (Accessed on: June 2024).

[56] Commission regulation (eu) 2016/631 of 14 april 2016 establishing a network code on requirements for grid connection of generators (text with eea relevance), Apr 2016. `http://data.europa.eu/eli/reg/2016/631/oj`.

[57] Commission regulation (eu) 2016/1388 of 17 august 2016 establishing a network code on demand connection (text with eea relevance), Aug 2016. `http://data.europa.eu/eli/reg/2016/1388/oj`.

[58] Commission regulation (eu) 2016/1447 of 26 august 2016 establishing a network code on requirements for grid connection of high voltage direct current systems and direct current-connected power park modules (text with eea relevance). Official Journal of the European Union, Aug 2016. `http://data.europa.eu/eli/reg/2016/1447/oj`.

[59] International Nuclear Safety Advisory Group. *Basic Safety Principles for Nuclear Power Plants: A Report*, volume 73. International Atomic Energy Agency, 1988.

[60] J Raeder. Safety and environmental assessment of fusion power (seafp). *EURFUBRUXII-217/95*, 1995.

[61] W Gulden and E Kajlert. Safety and environmental assessment of fusion power-long term programme (seal). *Summary Report of the SEAL Project European Commission DG XII Fusion Programme, Brussels*, 1999.

[62] D Maisonnier, I Cook, Sardain Pierre, Boccaccini Lorenzo, Bogusch Edgar, Broden Karin, Forrest Robin, Giancarli Luciano, Hermsmeyer Stephan, Nardi Claudio, et al. The european power plant conceptual study. *Fusion Engineering and Design*, 75:1173–1179, 2005.

[63] Neill Taylor, Dennis Baker, Sergio Ciattaglia, Pierre Cortes, Joëlle Elbez-Uzan, Markus Iseli, Susana Reyes, Lina Rodriguez-Rodrigo, Sandrine Rosanvallon, and Leonid Topilski. Updated safety analysis of iter. *Fusion engineering and design*, 86(6-8):619–622, 2011.

[64] International Nuclear Safety Advisory Group. *Defence in Depth in Nuclear Safety: INSAG-10: a Report*. International Atomic Energy Agency, 1996.

[65] E Gaio, A Ferro, A Lampasi, A Maistrello, M Dan, MC Falvo, F Gasparini, F Lunardon, A Magnanimo, M Manganelli, et al. Status and challenges for the concept design development of the eu demo plant electrical system. *Fusion Engineering and Design*, 177:113052, 2022.

[66] A. Monticelli. *Power Flow Equations*, pages 63–102. Springer US, Boston, MA, 1999.

[67] George J Anders. Probability concepts in electric power systems. 1989.

[68] Pei Zhang and Stephen T Lee. Probabilistic load flow computation using the method of combined cumulants and gram-charlier expansion. *IEEE transactions on power systems*, 19(1):676–682, 2004.

[69] Trevor Williams and Curran Crawford. Probabilistic load flow modeling comparing maximum entropy and gram-charlier probability density function reconstructions. *IEEE Transactions on Power Systems*, 28(1):272–280, 2012.

[70] Yan Chen, Jinyu Wen, and Shijie Cheng. Probabilistic load flow method based on nataf transformation and latin hypercube sampling. *IEEE Transactions on Sustainable Energy*, 4(2):294–301, 2012.

[71] N Soleimanpour and M Mohammadi. Probabilistic load flow by using nonparametric density estimators. *IEEE Transactions on Power systems*, 28(4):3747–3755, 2013.

[72] Antony Schellenberg, William Rosehart, and José Aguado. Cumulant-based probabilistic optimal power flow (p-opf) with gaussian and gamma distributions. *IEEE Transactions on Power Systems*, 20(2):773–781, 2005.

[73] Yue Yuan, Jianhua Zhou, Ping Ju, and Julian Feuchtwang. Probabilistic load flow computation of a power system containing wind farms using the method of combined cumulants and gram–charlier expansion. *IET renewable power generation*, 5(6):448–454, 2011.

[74] Mahdi Hajian, William D Rosehart, and Hamidreza Zareipour. Probabilistic power flow by monte carlo simulation with latin supercube sampling. *IEEE Transactions on Power Systems*, 28(2):1550–1559, 2012.

[75] Guido Carpinelli, Pierluigi Caramia, and Pietro Varilone. Multi-linear monte carlo simulation method for probabilistic load flow of distribution systems with wind and photovoltaic generation systems. *Renewable Energy*, 76:283–295, 2015.

[76] Alessandro Lampasi, Pietro Zito, Fabio Starace, Pietro Costa, Giuseppe Maffia, Simone Minucci, Elena Gaio, Vanni Toigo, Loris Zanotto, and Sergio Ciattaglia. The dtt device: Power supplies and electrical distribution system. *Fusion Engineering and Design*, 122:356–364, 2017.

[77] CR Lopes, C Terlizzi, R Romano, G Ala, G Zizzo, P Zito, S Bifaretti, V Bonaiuto, and A Lampasi. Guidelines and conceptual design of the grounding system of the dtt experimental facility. In *2022 IEEE 21st Mediterranean Electrotechnical Conference (MELECON)*, pages 489–494. IEEE, 2022.

[78] Stefano Panella, Maria Carmen Falvo, Sergio Ciattaglia, and Alessandro Lampasi. Demo fusion power plant: Preliminary sizing analysis of power system. In *2020 IEEE International Conference on Environment and Electrical Engineering and 2020 IEEE Industrial and Commercial Power Systems Europe (EEEIC / I&CPS Europe)*, pages 1–6, 2020.

[79] Sergio Ciattaglia, Maria Carmen Falvo, Alessandro Lampasi, and Matteo Proietti Cosimi. Energy analysis for the connection of the nuclear reactor demo to the european electrical grid. *Energies*, 13(9), 2020.

[80] Katsumi Okayama Joel Hourtoule François Sagot, Didier van Houtte and Inho Song. Optimizing iter power supplies operation through rami and standardization. *Fusion Science and Technology*, 60(1):134–138, 2011.

[81] Matteo Zaupa, Mauro Dalla Palma, Ivo Moscato, and Luciana Barucca. Balance of plant conceptual design of eu demo integrating different breeding blanket concepts. *Fusion Engineering and Design*, 200:114235, 2024.

[82] DIgSILENT. *DIgSILENT PowerFactory User Manual*. Gomaringen, Germany, 2020.

Acknowledgements

Come ogni avventura, anche questa è giunta al termine. È stato un percorso costellato di sfide, di momenti di sconforto, ma anche di grande calore umano. Se oggi sono una persona diversa rispetto a quando ho iniziato, molto lo devo a tutte le persone che hanno condiviso con me un pezzo della loro vita, rendendo il mio cammino meno arduo. A loro va la mia più sincera gratitudine.

I primi ringraziamenti vanno alla Prof.ssa Falvo, una figura sempre presente e disponibile, che con pazienza e competenza mi ha saputo guidare lungo il percorso di ricerca.

Un grazie speciale alla "gang" dell'ENEA: Alessandro, il mio storico tutor, sempre pronto a sistemare ogni poster, presentazione o articolo anche agli orari più improbabili; Roberto, per la sua competenza e, soprattutto, per la sua presenza comprensiva e silenziosa; Matteo Manganelli, sempre pronto a dare una mano a chi è in difficoltà.

Grazie a Stefano, per i consigli, le risate, le strigliate, le battute, il sostegno psicologico, le sfuriate e i balli scaramantici e propiziatori. Sei stato fondamentale sotto ogni aspetto e senza di te questi tre anni e oltre avrebbero avuto di certo meno sapore.

Grazie a Matteo Scanzano, per aver saputo risolvere con la sua pacatezza e senso pratico tutte le mie crisi interiori e lavorative.

Grazie a Riccardo, lontano ma vicino, per i messaggi estemporanei capaci di strapparmi un sorriso anche nelle giornate più opache.

Grazie a Sergio, che mi ha mostrato quanto la vita possa essere brillante se si ha il coraggio di superare i propri confini e affrontare ogni sfida con coraggio e tenacia.

Like every adventure, this one too has come to an end. It has been a journey full of challenges, moments of discouragement, but also great warmth. If I am a different person today than when I started, it is largely thanks to all the people who have shared a piece of their lives with me, making my path less arduous. To them goes my sincere gratitude.

My first thanks go to Professor Falvo, an ever-present and available figure who, with patience and expertise, has guided me along the research journey.

Thanks also to the "gang" at ENEA: Alessandro, my long-time tutor, always ready to fix every poster, presentation, or article even at the most improbable hours; Roberto, for his expertise and, above all, for his understanding and silent presence; Matteo Manganelli, always there to help those in need.

Thanks to Stefano, for the advice, the laughter, the scoldings, the jokes, the emotional support, the outbursts, and the propitiatory dances. You have been fundamental in every way and without you these three years and more would have certainly had less flavor.

Thanks to Matteo Scanzano, for having been able to solve all my inner and work crises with his calmness and practicality.

Thanks to Riccardo, far away but close, for the spontaneous messages that could always bring a smile to my face even on the gloomiest days.

Thanks to Sergio, who showed me how bright life can be if you have the courage to go beyond your limits and face every challenge with courage and tenacity.

Thanks to Simone, for the countless end-

Grazie a Simone, per le innumerevoli call infinite e tutto il sapere che mi hai trasmesso.

Grazie a Thomas per la tua curiosità contagiosa e professionalità.

Grazie ai "ragazzi di Monaco": Marco, Salvatore, Damiano, Pasquale, Sara e Giusy. Non ho abbastanza parole per esprimere quanto vi sia riconoscente per avermi permesso di essere me stessa e avermi fatto sentire accettata. Avete reso l'esperienza all'estero molto meno terrificante di quanto immaginassi all'inizio!

Grazie a Fabrizio, per la tua amicizia incondizionata. Sei una persona d'oro, oltre ad essere il mio tesista preferito!

Grazie a Virginio, il mio papà d'adozione, per i tuoi "high five", i "Marzy Panzy" random e tutte le risate che ancora riesci a strapparmi tra le lacrime. Grazie perché credi in me più di quanto non faccia io stessa.

Grazie a Valerio, per aver alleggerito i miei pomeriggi sulle note delle canzoni arrangiate apposta per me. Sei un maestro di chitarra eccezionale e una persona sensibile e meravigliosa.

Grazie a Botond, per tutta la gioia che hai saputo regalarmi in maniera del tutto inaspettata e travolgente.

Grazie a Bianca ed Erika, il mio porto sicuro, il mio riparo nella tempesta. Grazie per tutto il conforto che mi avete dato, per esserci state quando avevo bisogno e anche quando non ne avevo bisogno. Vi adoro.

Grazie a Luca, per avermi tenuto a lungo per mano e aver avuto il coraggio di lasciarmi andare e spiegare le ali. Se le nostre strade si incroceranno nuovamente, spero che le esperienze vissute ci avranno resi entrambi più forti.

Grazie alla mia famiglia che, pur non condividendo tutte le mie scelte, non ha mai mancato di farmi sentire il suo affetto e il suo amore.

Grazie, grazie, grazie.

less calls and all the knowledge you shared with me.

Thanks to Thomas for your contagious curiosity and professionalism.

Thanks to the "Munich guys": Marco, Salvatore, Damiano, Pasquale, Sara, and Giusy. I don't have enough words to express how grateful I am to you for allowing me to be myself and for making me feel accepted. You made the experience abroad much less terrifying than I had initially imagined!

Thanks to Fabrizio, for your unconditional friendship. You are a golden person, in addition to being my favorite thesis student!

Thanks to Virginio, my adoptive dad, for your "high fives", random "Marzy Panzy" moments, and all the laughter you still manage to bring out of me through tears. Thank you for believing in me more than I do in myself.

Thanks to Valerio, for lightening up my afternoons with the songs you arranged just for me. You are an exceptional guitar teacher and a sensitive and wonderful person.

Thanks to Botond, for all the joy you have brought into my life in such an unexpected and overwhelming way.

Thanks to Bianca and Erika, my safe harbor, my shelter in the storm. Thank you for all the comfort you have given me, for being there when I needed you and even when I didn't. I adore you.

Thanks to Luca, for holding my hand for so long and having the courage to let me go and spread my wings. If our paths cross again, I hope the experiences we have lived will have made us both stronger.

Thanks to my family who, even without sharing all my choices, never failed to make me feel their love and affection.

Thank you, thank you, thank you.